Deep–Sea Research II 189-190 (2021) 104951

Contents lists available at ScienceDirect

Deep-Sea Research Part II

journal homepage: www.elsevier.com/locate/dsr2

Evaluating the impact of climate and demographic variation on future prospects for fish stocks: An application for northern rock sole in Alaska

André E. Punt [a,*], Michael G. Dalton [b], Wei Cheng [c,d], Albert J. Hermann [c,d], Kirstin K. Holsman [b], Thomas P. Hurst [e], James N. Ianelli [b], Kelly A. Kearney [c,b], Carey R. McGilliard [b], Darren J. Pilcher [c,d], Matthieu Véron [a]

[a] School of Aquatic and Fishery Sciences, University of Washington, Seattle, WA, United States
[b] Alaska Fisheries Science Center, National Marine Fisheries Service, NOAA, 7600 Sand Way Point Way, NE, Seattle, WA, United States
[c] Cooperative Institute for Climate, Ocean, And Ecosystem Studies, University of Washington, Seattle, WA, United States
[d] Pacific Marine Environmental Laboratory, Oceans and Atmospheric Research, National Oceanic and Atmospheric Administration, Seattle, WA, United States
[e] Alaska Fisheries Science Center, National Marine Fisheries Service, NOAA, Hatfield Marine Science Center, Newport, OR, USA

ARTICLE INFO

Keywords:
Bayesian methods
Climate
Demographics
Environment
Maximum economic yield
Northern rock sole

ABSTRACT

Climate-enhanced stock assessment models represent potentially vital tools for managing living marine resources under climate change. We present a climate-enhanced stock assessment where environmental variables are integrated within a population dynamics model assessment of biomass, fishing mortality and recruitment that also accounts for process error in demographic parameters. Probability distributions for the impact of the associated environmental factors on recruitment and growth can either be obtained from Bayesian analyses that involve fitting the population dynamics model to the available data or from auxiliary analyses. The results of the assessment form the basis for the calculation of biological and economic target and limit reference points, and projections under alternative harvest strategies. The approach is applied to northern rock sole (*Lepidopsetta polyxystra*), an important component of the flatfish fisheries in the Eastern Bering Sea. The assessment involves fitting to data on catches, a survey index of abundance, fishery and survey age-compositions and survey weight-at-age, with the relationship between recruitment and cold pool extent and that between growth increment in weight and temperature integrated into the assessment. The projections also allow for an impact of ocean pH on expected recruitment based on auxiliary analyses. Several alternative models are explored to assess the consequences of different ways to model environmental impacts on population demography. The estimates of historical biomass, recruitment and fishing mortality for northern rock sole are not markedly impacted by including climate and environmental factors, but estimates of target and limit reference points are sensitive to whether and how environmental variables are included in stock assessments and projections.

1. Introduction

The US approach to setting management controls (and those of most developed countries) is predicated on the assumption of a stationary system, in particular that the levels of productivity inferred from stock assessments based on historical data are appropriate for the future.[1] However, the effects of global climate change present an obvious challenge to this paradigm (e.g., Litzow et al., 2018). Anthropogenic climate change has altered climate processes that structure marine conditions (Meredith et al., 2019). Consequently, multiple US marine systems increasingly demonstrate unidirectional shifts in oceanographic conditions such as surface and water column warming, loss of sea ice, altered salinity and stratification, changes to circulation patterns, increases in low oxygen zones, and altered ocean pH and carbonate dynamics (Breitburg et al., 2018; Claret et al., 2018; Meredith et al., 2019; Howard et al., 2020). These changes are most pronounced in Arctic systems where warming is twice the rate of the global average and where transformation of entire ecosystems may be underway (Meredith et al., 2019; Huntington et al., 2020). Climate change has also induced recent marine heat waves, i.e., sudden severely anomalous warm conditions

* Corresponding author.
E-mail address: aepunt@uw.edu (A.E. Punt).

[1] Although the US Magnusson-Stevens Act states that reference points such as B_{MSY} and F_{MSY} should be based on "prevailing environmental conditions".

https://doi.org/10.1016/j.dsr2.2021.104951
Received 31 March 2021; Received in revised form 9 July 2021; Accepted 18 July 2021
Available online 24 July 2021
0967-0645/© 2021 The Author(s). Published by Elsevier Ltd. This is an open access article under the CC BY-NC-ND license (http://creativecommons.org/licenses/by-nc-nd/4.0/).

that can persist for months to years (Frölicher et al., 2018; Laufkötter et al., 2020). Biological responses to altered conditions and marine heatwaves can be immediate or lag impacts, and manifest over multiple years (Meredith et al., 2019; Smale et al., 2019; Turner et al., 2020). Observed responses to climate change in the North Pacific include rapid redistribution of populations (Spies et al., 2020; Stevenson and Lauth, 2019), which can impact the overlap of predator and prey resources (Siddon et al., 2013; Spencer et al., 2016; Carroll et al., 2019), alter fishery access (Stevenson and Lauth, 2019), and increase the risk of fishery closures due to bycatch or entanglement (Santora et al., 2020).

Climate-driven changes to marine conditions have also induced sudden increases in physiological processes and metabolic demand with direct non-lethal impacts on growth and fish condition (Barbeaux et al., 2020; Dahlke et al., 2020) and reproduction, as well as altered survival rates due to cascading impacts of food web alterations (Mueter et al., 2020; Piatt et al., 2020), physiological stress, or exposure to harmful algal blooms and disease favoured under warmer conditions (IPCC, 2019; Lefebvre et al., 2016), the latter of which can also directly lead to fishery closures (e.g., Fisher et al., 2021). Observed impacts and responses are anticipated to become commonplace over the next 20–30 years, with increasing alterations projected under the highest atmospheric CO_2 emission scenarios (Deutsch et al., 2015; IPCC, 2019; Oliver et al., 2018). Accounting for climate-driven ecosystem alterations is increasingly considered to be necessary to effectively manage living marine resources (Holsman et al., 2019; Karp et al., 2019; Narita et al., 2020).

The fish and invertebrate fisheries of the Eastern Bering Sea (EBS), Alaska, are amongst the world's largest and are also major drivers of revenue and employment for the State of Alaska and the Pacific Northwest. The largest fisheries by volume in the region are those for Alaska (or walleye) pollock (*Gadus chalcogrammus*) and Pacific cod (*Gadus macrocephalus*), with the fisheries for crab and sablefish (*Anoplopoma fimbria*) amongst the most valuable. Climate change impacts are particularly evident in this area. A seasonally sea-ice driven system (Sigler et al., 2016; Thorson et al., 2021), warming over the past 30 years combined with loss of winter sea ice has altered the productivity and distribution of species across the system (Huntington et al., 2020; Stevenson and Lauth, 2019). Sea ice extent and duration in 2018 was the lowest in the last 5500 years and may lag atmospheric CO_2 levels by a few decades according to a recent isotopic enabled model simulation study (Jones et al., 2020). Further, climate projections indicate that Bering winter sea ice may disappear by mid-to late-century under high global atmospheric CO_2 scenarios (Wang and Overland, 2015; Wang et al., 2018; Hermann et al., 2019).

Recent observations of climate impacts and future projections of anticipated change indicate that the EBS is likely to be strongly impacted by future climate change (Meredith et al., 2019, this issue). In particular, results from earth system models downscaled to local conditions already show evidence of aragonite undersaturation in some regions of the Bering Sea (Pilcher et al., 2019). Projections based on the 5th Coupled Model Intercomparison Project (CMIP5) models show bottom temperatures will increase by 5 °C by 2100 under Representative Concentration Pathway (RCP) 8.5 (Hermann et al., 2019), with consequences for a range of taxa (e.g., Holsman et al., 2020; Reum et al., 2020; Whitehouse et al., 2021; Szuwalski et al., 2021). There will undoubtedly be regional variation in the effects of global climate change even within Alaskan marine areas, but there is a need to understand the consequences of changing environmental conditions (e.g., pH and temperature) on stock trends, catches and revenues to assist decision makers with their strategic planning.

Decision making for many federally managed US fisheries involves the application of harvest control rules that determine an Overfishing Limit (OFL; the catch corresponding to a fishing mortality rate according to an F_{MSY} control rule) and an Acceptable Biological Catch (ABC; the OFL as reduced to account for scientific uncertainty), with the Annual Catch Limit (ACL), i.e., the Total Allowable Catch (TAC), set equal to or less than the ABC. This approach to management decision making has the advantage that it separates the biological aspects of decision making (i.e., determination of stock status, calculation of the OFL and quantification of the level of scientific uncertainty) from the policy aspects (e.g., the amount by which the OFL should be reduced to account for scientific uncertainty, and how the TAC should be set given the ABC; Ralston et al., 2011). Specification of OFLs, ABCs, and ACLs within the US varies regionally in response to local conditions, including data availability; some approaches being very formulaic and others much less so (Privitera-Johnson and Punt, 2020). Specification of OFLs and ABCs are fundamentally biological concepts, and guidelines for setting ACLs leading to TACs rarely explicitly reflect economic considerations.[2]

Several analyses (some model-based, others not) have been undertaken to understand the direct (e.g., on survival and growth) consequences of changes in pH over time from ocean acidification on the stocks and fisheries of the North Pacific and other regions within the US (e.g., Kaplan et al., 2010; Moore, 2014; Cooley et al., 2015; Punt et al., 2014; 2016; 2020; Seung et al., 2015; Colt and Knapp, 2016; Swiney et al., 2016; Rheuban et al., 2018). Within the EBS, the focus for investigations of ocean acidification using population dynamics models fitted to monitoring data have been crab stocks (e.g., Punt et al., 2014, 2016, 2020), for which integrated bio-economic models in which larval and juvenile dynamics are driven by ocean pH have been developed for EBS Tanner crab (*Chionoecetes bairdi*) and Bristol Bay red king crab (*Paralithodes camtschaticus*). These analyses indicate that expected catches and net operating profits will be lower in the future (generally after 2040) given the estimated negative effects of ocean acidification on larval and juvenile survival.

Although much focus for the direct impacts of ocean acidification has been on invertebrates, fish are also likely to be impacted both directly by ocean acidification and other consequences of ocean environmental change (and indirectly through changes in demographics, predation, food availability and quality, etc). This paper focuses on northern rock sole (*Lepidopsetta polyxystra*), an important component (annual average catch of 41,414 t during 2012–2019; Supplementary Appendix C) of the flatfish fisheries in the EBS. This species was selected because several studies have detected impacts of environmental factors on demographic parameters and processes. Specifically, Hurst et al. (2016, 2017) found a weak effect of pH on larval survival, Cooper et al. (2019) found a relationship between recruitment and (i) the portion of the nursery area (as defined in Cooper et al., 2014) for northern rock sole covered by various low temperature values (1.5 °C was selected based on their model fits) and (ii) a categorical index of winds during the larval period for northern rock sole. Matta et al. (2010) and Hurst and Abookire (2006) found an effect of temperature on growth rate for rock sole.

The broad aim of the paper is to integrate the effects of environmental change into age-structured stock assessment models and hence the provision of climate-informed management advice in the form of reference points and how they may change over time. Specifically, we extend the stock assessment for northern rock sole (McGilliard et al., 2020) with a method that integrates the estimation of temperature effects on growth (e.g., Plagányi, 2007). Second, a threshold temperature within the main nursery area is modelled as an effect on recruitment. Finally, an estimated relationship between larval survival and pH obtained by Hurst et al. (2016) adds another impact on recruitment.

This integrated model is then linked to a model of profit, and used to calculate biological and economic reference points (MSY, F_{MSY}, Maximum Economic Yield (MEY), and F_{MEY}), information that could be used when TACs are selected. Some of the relationships are quite weak so the calculations account for estimation uncertainty using Bayesian

[2] Few countries explicitly account for economic factors when setting management reference points, a notable exception being Australia for which the biomass at which Maximum Economic Yield (MEY) is achieved is the target reference point (Dichmont et al., 2010).

methods, and hence the results are expressed as probability distributions. The sensitivity of the results to inclusion of a subset of the environment-demographic parameter relationships is examined to assess the impact of each factor in turn as well as in combination.

The results of the paper provide key climate-informed advice for decision-makers and stakeholders in the EBS. This contribution is part of a collection of papers conducted as part of the Alaska Climate Integrated Modeling (ACLIM) research program (Hollowed et al., 2020). This program utilizes a multi-model approach to project the implications of climate change on the EBS shelf and slope ecosystems. The project seeks to use the multi-model approach to identify sources of structural, process and scenario uncertainty. Analysts project the implications of changing climate under current and alternative fishing strategies to inform managers and the public of the projected impacts of climate change while evaluating the performance of proposed adaptation strategies with respect to achieving the goals and objectives of US National Standards for Sustainable Fisheries Management (Holsman et al., 2020).

2. Methods

Fig. 1 provides an overview of how the environmental drivers and environmental variation are integrated into the stock assessment, the calculation of reference points, and the biological and economic projections under alternative harvest strategies. The environmental drivers considered in the analyses are (a) the size of the cold pool and its negative effects on the survival of settled juveniles in their nursery area, (b) the positive effects of bottom temperature on annual weight increment, and (c) the negative effect of ocean acidification on larval survival. Random variation in recruitment and the cohort-specific values for growth parameters are also considered to allow the model to fit the available data beyond what is possible given the environmental drivers.

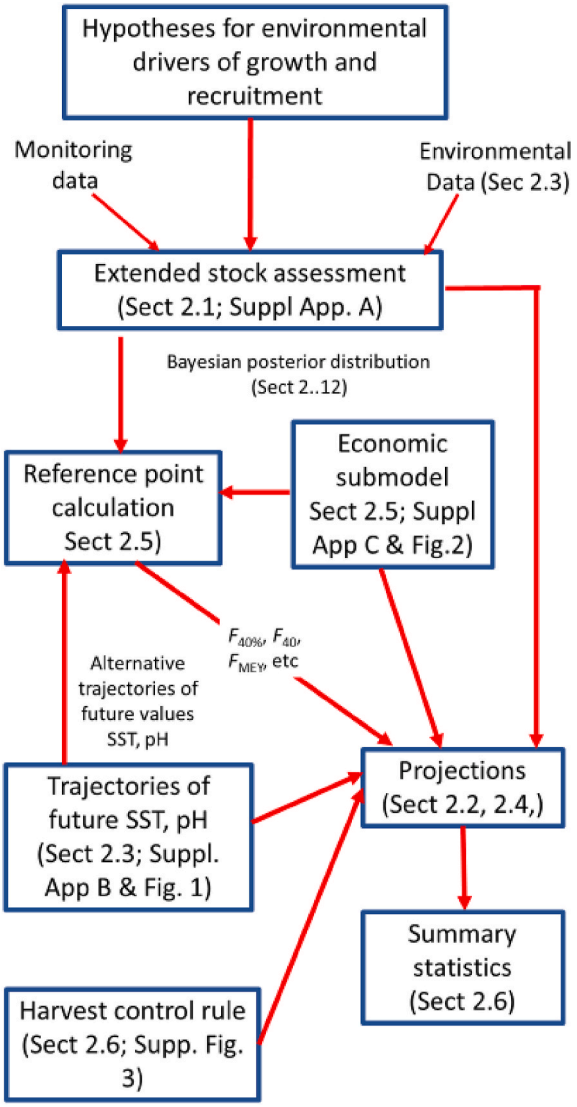

Fig. 1. Flowchart of the approach for evaluating the impact of climate and demographic variation on estimates of reference points and management performance.

2.1. Population dynamics model

The population dynamics model used as the basis for the forecasts is largely based on the model used in the most recent stock assessment for Bering sea northern rock sole (McGilliard et al., 2020)[3] but with some modifications, most notably the methodology for representing growth. The population dynamics model is age-structured (ages-classes 1–20; the last of which is a plus-group), and considers the years 1975–2020. Projections consider the years 2020 onwards, where the mortality for age-0 animals (pre-recruits) can be a function of various covariates including temperature and ocean pH, while length-at-age can vary over time and be driven by environmental variables such as temperature. The projections start in 2020 (rather than 2021) because the assessment does not estimate a recruitment for 2020.

2.2. Basic dynamics

The basic dynamics are governed by the equation:

$$N^s_{t+1,a} = \begin{cases} 0.5R_{t+1} & \text{if } a = 1 \\ N^s_{t,a-1}e^{-Z^s_{t,a-1}} & \text{if } 1 < a < A \\ N^s_{t,A-1}e^{-Z^s_{t,A-1}} + N^s_{t,A}e^{-Z^s_{t,A}} & \text{if } a = A \end{cases} \quad (1)$$

where $N^s_{t,a}$ is the number of animals of sex s and age a at the start of year t, R_t is the recruitment (at age 1) during year t, A is the plus-group age, $Z^s_{t,a}$ is the total mortality for animals of sex s and age a during year t:

$$Z^s_{t,a} = M^s + F^s_{t,a} \quad (2)$$

M^s is the rate of natural mortality for animals of sex s aged one and older, $F^s_{t,a}$ is the fishing mortality rate for animals of sex s and age a during year t:

$$F^s_{t,a} = S^s_{t,a}F_t \quad (3)$$

$S^s_{t,a}$ is selectivity as a function of age, sex and time:

$$S^s_{t,a} = \left(1 + \exp\left(s^s e^{\omega^{s,s}_t}\left(a - a^s_{50}e^{\omega^{a_{50},s}_t}\right)\right)\right)^{-1} \quad (4)$$

where s^s is the reference selectivity slope parameter for sex s, a^s_{50} is the reference selectivity intercept parameter for sex s, $\omega^{s,s}_t$ is the annual selectivity slope deviation for sex s, $\omega^{a_{50},s}_t$ is the annual selectivity intercept deviation for sex s, F_t is the fully-selected fishing mortality during year t:

$$F_t = \widetilde{F}e^{\delta_t} \quad (5)$$

$\widetilde{F}$ is the reference level of fully-selected fishing mortality, and δ_t is the fishing mortality deviation for year t.

The total catch in mass is given by:

[3] The 2020 assessment set weight-at-age to the actual survey observations whereas the model of this paper treats the weight-at-age observations as data and models length-at-age using parametric functions.

$$C_t = \sum_s \sum_{a=1}^{A} w_{t,a}^s \frac{F_{t,a}^s}{Z_{t,a}^s} N_{t,a}^s \left(1 - e^{-Z_{t,a}^s}\right) \quad (6)$$

where $w_{t,a}^s$ is the mean weight of an animal of sex s and age a during year t. Mean weights-at-age were assumed to vary depending on temperature and the initial size of each cohort:

$$w_{t,a}^s = \begin{cases} \alpha^s \left(L_{t,1}^s\right)^{\beta^s} & \text{if } a = 1 \\ w_{t-1,a-1}^s + \left\{\alpha^s \left(L_{t,a}^s\right)^{\beta^s} - \alpha^s \left(L_{t-1,a-1}^s\right)^{\beta^s}\right\} e^{\eta T_t} & \text{otherwise} \end{cases} \quad (7)$$

where $L_{t,a}^s$ is the expected length of an animal of sex s and age a during year t:

$$L_{t,a}^s = \ell_\infty^s e^{\varphi_{t-a}^1} \left(1 + \left(L_1^s e^{\varphi_{t-a}^2} - 1\right) e^{-\kappa^s e^{\varphi_{t-a}^3}(a-1)}\right) \quad (8)$$

ℓ_∞^s, κ^s are the reference values for the von Bertalanffy growth parameters for sex s, L_1^s is the reference value for the length of an age-1 animal of sex s relative to ℓ_∞^s, α^s, β^s are the length-weight parameters for sex s, T_t is the bottom temperature index during year t (normalized to the mean over 1974–2019), φ^1, φ^2, φ^3 are the parameters that determine how ℓ_∞^s, initial length and spawning biomass during κ^s vary over time ($\varphi_t^1 \sim N(0; \sigma_{\ell_\infty}^2)$; $\varphi_t^2 \sim N(0; \sigma_{L_1}^2)$; and $\varphi_t^3 \sim N(0; \sigma_\kappa^2)$); $\sigma_{\ell_\infty}^2, \sigma_{L_1}^2, \sigma_\kappa^2$ determine the extent to which the von Bertalanffy parameters vary over time; and η is the parameter relating the bottom temperature to growth increment in weight (growth is time-invariant for $\varphi^1 = \varphi^2 = \varphi^3 = \eta = 0$).

The spawning biomass during year t (at the start of February after 1/12 of total mortality), $\widetilde{S}_t$ is:

$$\widetilde{S}_t = \sum_{a=1}^{A} m_a \, w_{t,a}^{\mathrm{f}} \, N_{t,a}^{\mathrm{f}} \, e^{-Z_{t,a}^{\mathrm{f}}/12} \quad (9)$$

m_a is the proportion of animals of age a that are mature.

Following Cooper et al. (2019) the number of age-1 animals at the start of year t was modelled to be related to the proportion of the nursery ground colder than 1.5 °C ("cold pool extent"), i.e.:

$$R_t = \overline{R} e^{\gamma_1 C_{t-1}} e^{\varepsilon_t - \sigma_R^2/2} \quad \varepsilon_t \sim N\left(0; \sigma_R^2\right) \quad (10)$$

where $\overline{R}$ is median recruitment, C_t is the cold pool extent during year t (normalized to the mean over 1974–2019), γ_1 is the parameter related to cold pool size, and σ_R is the extent of additional variation in recruitment about median recruitment.

2.3. Parameter estimation

The parameters of the population dynamics model (see Supplementary Table A.2 for the estimable parameters) were estimated by fitting the model to catch data, a survey index of abundance, fishery and survey age-composition data, and survey weight-at-age data (Supplementary Appendix A). The estimation was conducted within the Bayesian framework, with most of the priors specified to be uniform (Supplementary Table A.2). The samples from the posterior distributions for the parameters of the population dynamics model were obtained using the Markov chain Monte Carlo (MCMC) algorithm included in AD Model Builder (Fournier et al., 2012). The rate of natural mortality, M, was not estimated but was rather pre-specified at the value used when conducting the most recent stock assessment (0.15yr^{-1} for both sexes).

2.4. Projections

Projections were conducted for each draw from the posterior distribution. The projections extend the assessment period (1975–2020) and allow for the possibility of expected recruitment being related to forecasted cold pool extent and to pH (the relationship between larval survival and pH [and impact on age-1 abundance] was modelled based on the results of experiments conducted by Hurst et al., 2016; Supplementary Appendix B),[4] with growth impacted by trends in temperature, i.e.: for recruitment

$$R_t = \overline{R} e^{\gamma_1 C_{t-1} + \gamma_2 P_{t-1}} e^{\varepsilon_t - \sigma_R^2/2} \quad \varepsilon_t \sim N\left(0; \sigma_R^2\right) \quad (11)$$

where P_t is the pH (normalized to average zero over 2006–2020) during year t, and γ_2 is the parameter related to pH (Supplementary Appendix B). $\overline{R}$ is mean recruitment when calculating references points and median recruitment when conducting stochastic forecasts.

In the assessment, fishery selectivity varies inter-annually subject to a prior constraint (see Equation A.10). For simplicity, selectivity in the projections is taken to be the average over the last five years of assessment (2016–2020).

2.5. Environmental data

Environmental data (cold pool extent, temperature and pH; Supplementary Fig. 1) were derived from a regional hydrodynamic model of the Bering Sea, and represent average conditions during the growing season (May-June-July-August). These indices were selected based on the results of previous analyses relating population dynamic parameters to environmental indices (see Section 1). The model, Bering10 K, is an implementation of the Regional Ocean Modeling System (ROMS) with a domain covering the Bering Sea with 10-km horizontal resolution (Hermann et al., 2016; Kearney et al., 2020). For this study, we extracted bottom temperature time series from two simulations, both part of the larger ACLIM suite. The first of these was a 30-layer hindcast simulation spanning 1970–2020; this simulation was forced by surface and lateral boundary conditions from reanalysis data products, and it has been shown to replicate observed spatiotemporal variability in surface and bottom temperatures across the EBS shelf (Kearney et al., 2020; Kearney, 2021).[5] The second simulation was a 10-layer long-term projection spanning 2006–2100 (Hermann et al., 2019); this simulation downscaled the GFDL-ESM2M model (Dunne et al., 2013) under the RCP8.5 emission scenario from CMIP5 (Taylor et al., 2012). From both simulations, surface temperature indices were calculated by averaging vertically over the top 5 m relative to the model's free surface and horizontally over the southeastern Bering Sea shelf polygon (Supplementary Fig. 1). Cold pool indices were defined as the fraction of the nursery area polygon (see Cooper et al., 2019) with a bottom temperature less than 1.5 °C, with bottom temperature defined as the mean temperature over the bottom 5 m of the water column.

The pH data indices were produced from a 30-layer ROMS downscaling of the GFDL-ESM2M model under RCP 8.5, which included carbonate chemistry additions to the Bering10 K BESTNPZ model (Pilcher et al., 2019; Kearney et al., 2020). pH was calculated from model output of temperature, salinity, total alkalinity, and dissolved inorganic carbon using CO2SYS (Lewis and Wallace, 1998). Observational data for pH over the historical assessment period are relatively scarce, though the model has previously demonstrated skill in reproducing carbonate variables under historical hindcast conditions (Pilcher et al., 2019). Similar to temperature, the pH indices were averaged vertically over the top 5 m, and horizontally using a spatially-weighted mean for the rock sole nursery ground. Lanksbury et al. (2007) observed northern rock sole larvae distributed throughout the water column, and reported diel and depth-related effects. The highest larval abundances

[4] Supplementary Appendix B also provides a posterior for the parameter that relates CO_2 to larval survival, but in the absence of projections of CO_2 levels, all the analyses are based on projections of pH.

[5] See Kearney et al. (2020) for full details of the simulation's input forcing and parameterization.

during the day were observed between 10 and 30 m, and at night, between 0 and 10 m, and between 30 and 50 m (Lanksbury et al., 2007, Fig. 8). Averaging over a greater depth range is possible, but we lack a larval vertical distribution for the nursery area in Cooper et al. (2014), which is north of Bristol Bay. The larval vertical distribution reported in Lanksbury et al. (2007) was observed near the Alaska Peninsula and Unimak Island.

2.6. Scenarios and model selection

The scenarios we examined (models 0–9; Table 1) relate to which processes are impacted by environmental change. Specifically, the null model (0) assumes that growth is time-invariant, recruitment is equal to a mean with log-normal variance,[6] and larval survival is independent of ocean pH. The remaining models allow for various combinations of these factors, with the two variants of the full model allowing all three processes to be impacted by environmental factors. Results are not provided for models in which more than one von Bertalanffy growth parameter varies over time. This is because the MCMC algorithm did not converge for such models, likely due to annually varying growth parameters being confounded.

2.7. Reference points

The reference points are computed at the start of each decade from 2020 to 2090 to reflect the impact of environmental drivers on recruitment and growth (see Table 2 for the options considered). The reference points are:

- $F_{35\%}$ and $F_{40\%}$ - the fully-selected fishing mortality rates corresponding to 35 % and 40 % reductions in spawning biomass-per-recruit for a cohort (the value of Equation (9) in equilibrium divided by R_0) compared to the spawning biomass-per-recruit when there is no fishing. Weight-at-age is calculated for the year concerned (y_*) or the average weight-at-age for years y_*-4 to y_*.
- F_{35} and F_{40} - the fully-selected fishing mortality rates corresponding to 35 % and 40 % reductions in spawning biomass compared to unfished spawning biomass where spawning biomass is computed for the year concerned (y_*) or the average weight-at-age for year y_*-4 to y_*. Recruitment is the expected recruitment for year y_*, the average of the expected recruitment for years y_*-4 to y_*, or the "dynamic B_0" estimate of recruitment (A'mar et al., 2009; Ianelli et al., 2011):

$$\overline{R}_y = \sum_{a=1}^{A} w^{f}_{y-a+1,a}\, m_a\, R_{y-a+1} e^{-(a-1)M} \Big/ \sum_{a=1}^{A} w^{f}_{y-a+1,a}\, m_a\, e^{-(a-1)M} \quad (12)$$

The weight-at-age used to compute unfished spawning biomass is based on the reference values for the growth parameters, and $\overline{R}$ is set to an estimate mean recruitment.)[7,8]

- F_{MSY}, MSY, B_{MSY}/B_0 - the fully-selected fishing mortality rate, yield and spawning biomass expressed relative to unfished spawning biomass corresponding to maximum sustainable yield, i.e. the value of Eqn (6) in equilibrium.
- F_{MEY}, C_{MEY}, B_{MEY}/B_0, MEY, the fully-selected fishing mortality rate, yield, spawning biomass expressed relative to unfished spawning biomass, and profit (Eqn (13)) when profit is maximized in equilibrium. In this case, profit is determined by decomposing the northern rock sole sector from profits of the Amendment 80 fishery in the Bering Sea, as calibrated to benchmark data for catch, effort, cost, and revenue (see Supplementary Appendix C):

$$\pi(F_t) = pC(F_t) - c\,E_t \quad (13)$$

where $p = \$949$/t (Supplementary Table C.3; Supplementary Fig. C.2) is price-per-unit catch biomass for the northern rock sole sector, $C(F_t)$ is the catch during year t given a fully-selected fishing mortality of F_t, $c = \$56{,}606$/day (Supplementary Table C.3) is the cost per unit effort, E_t is the effort during future year t, as represented by the total number of days fishing for northern rock sole in the Bering Sea (Supplementary Fig. 2; Supplementary Fig. C.1). Effort is related to fishing mortality according to $E_t = F_t/q$, where q is a catchability coefficient. Cost includes daily-equivalent expenditures for vessel capital, labor, bait, equipment, food, fuel, packaging materials, and taxes (Supplementary Fig. C.3).

For calculating reference points, future (post-2020) values for ℓ^s_∞, L^s_1, and κ^s were alternatively set to their lower 5 %, median or upper 5 % percentiles. The choice of the lower and upper 5 % percentiles is illustrative and other percentiles could have been chosen to identify the effect of persistent changes in growth parameters. The values for weight-at-age during 2020 were estimated within the assessment so the 2020 weights-at-age were set to the estimates and changes in ℓ^s_∞, L^s_1, and κ^s were implemented starting with the 2021 cohort. Thus, for example, the weights-at-age in 2030 for ages 1–10 were based on assumptions about future ℓ^s_∞, L^s_1, and κ^s while those for ages 11+ were based on projecting the estimated weights-at-age for 2020 forward 10 years.

The reference points are based on expected (mean) recruitment rather than median recruitment because the calculations are deterministic, i.e. $\sigma_R = 0$ in Equation (11) (and the estimate of $\overline{R}$ is hence lower than mean recruitment). Consequently, the value for unfished recruitment used when computing reference points ($\overline{R}$ in Equation (11)) was the average recruitment (over 1976–2020) before account was taken of enviromental factors so that the value for recruitment is an estimate of expected recruitment.

2.8. Impacts of alternative harvest strategies

Models 0, 8 and 9 are projected forward under 29 harvest strategies. The first 28 of these are based on two broad classes of harvest strategy that set the annual fishing mortality rate for each future year according to: 1) constant fishing mortality and 2) the 40-5 harvest control rule (Supplementary Fig. 3). Several choices are considered for how to parameterize these two broad classes of harvest strategy. Specifically, the values for the constant fishing mortality/the maximum fishing mortality for the 40-5 harvest strategy within each broad strategy are taken to the posterior medians for $F_{40\%}$, F_{40}, or F_{MEY} in 2020 and 2090 based on models 0, 8 and 9 when weight-at-age is set to the average weight-at-age for the five years prior to the year concerned and recruitment is based on the dynamic B_0 approach.[9] Unfished biomass is set to the posterior median so that the resulting catches correspond to Acceptable Biological Catches (Anon., 2020). The final (reference) harvest strategy involves setting the future fishing mortality equal to average over the last five years included in the assessment (2016–20) for the model on which the projections are based (i.e., the average fishing mortality differs among the projections based on models 0, 8 and 9). The models on which the projections are based are fully crossed with the

[6] The variance in recruitment about expected recruitment, quantified by σ_R, is due to unmodelled environmental factors.

[7] The reference points are based on expected (mean) recruitment rather than median recruitment because the calculations are deterministic, i.e. $\sigma_R = 0$ and the estimate of $\overline{R}$ is hence lower than the mean recruitment.

[8] We use the term "dynamic B_0" for consistency with its usage in the literature but given the number of age-classes in the northern rock sole model and the fairly low rate of natural mortality, "dynamic B_0" is less "dynamic" than a 5-year average.

[9] There are only four harvest strategies based on model 0 because $F_{40\%} = F_{40}$ for model 0 and because the values for the reference points for 2020 are the same as those for 2090 for this model; there are 12 harvest strategies for models 8 and 9.

Table 1
The alternative models. Note that the assessment results are not impacted by assumptions about larval survival because that variable only relates to the projections (and calculation of reference points). The final two columns are the value of the objective function at the maximum of the posterior density function and the estimate of extent of observation error associated with the weight-at-age information.

Model No	Annual variation in growth parameters	SST impact on growth increment	Nursery ground impact on recruitment	pH impact on recruitment[1]	Objective function	$\widetilde{\sigma}$
0 (null)	No	No	No	No	3006.99	1.845
0*	No	No	No	Yes	3006.99	1.845
1	No	Yes	No	No	2995.96	1.832
2	L_1	Yes	No	No	2801.39	1.650
3	κ	Yes	No	No	2716.88	1.590
4	ℓ_∞	Yes	No	No	2706.18	1.605
5	No	No	Yes	Yes	3005.52	1.845
6	No	Yes	Yes	Yes	2994.52	1.832
7	L_1	Yes	Yes	Yes	2800.08	1.650
8	κ	Yes	Yes	Yes	2715.66	1.590
9	ℓ_∞	Yes	Yes	Yes	2704.95	1.605

1:Projections only.

Table 2
Options for computing fishing mortality-based reference points for year y.

	$F_{35\%}$	F_{35}, F_{MSY}, F_{MEY}
Recruitment		
Unfished	1	R_0
Fished	1	Year y; average years y-4 to y; dynamic B_0
Weight-at-age		
Unfished	As for fished	Based on reference values
Fished growth parameters	lower 5 %; median; upper 5 %	lower 5 %; median; upper 5 %
Temperature impact on growth increment	Year y; average years y-4 to y	Year y; average years y-4 to y

models used to set the reference points on which the harvest strategies are based (i.e. 29 x 3 projections in total).

The performance metrics used to summarize the results of the projections are:

- probability that the spawning biomass drops below 17.5 % of the unfished biomass (i.e., the probability of stock dropping below the overfished threshold, Anon, 2020);
- probability that annual profit is negative;
- median and 90 % intervals (over draws from the posterior) for the average catch;
- median and 90 % intervals (over draws from the posterior) for the average profit; and
- median and 90 % intervals (over draws from the posterior) for the annual average variation in catches, i.e.:

$$AAR_s = \sum_{y=2020}^{2099} \left| C_{s,y} - C_{s,y-1} \right| \Big/ \sum_{y=2019}^{2098} C_{s,y} \tag{14}$$

where AAR_s is the annual average variation in catches for MCMC draw s, and $C_{s,y}$ is the catch for year y and draw s.

The first four performance metrics are computed for 2020–29 (first 10 years of the projection period), and 2090–99 (last 10 years of the projections) while the AAR is computed over the entire projection period.

3. Results

3.1. Including environmental factors in the stock assessment

3.1.1. Maximum posterior density estimation and model selection

The best fit of the model to the data (based on the parameter values corresponding to the maximum of the posterior density function) improves when allowance is made for the impact of cold pool extent on recruitment, the impact of temperature on growth increment in weight, and annual variability in the parameters of the von Bertalanffy growth function (Table 1 [10]). The magnitude of improvement in fit (as quantified by the change in the objective function) is relatively small for recruitment (a reduction in the objective function of <1.5 units). In contrast, the fit to the survey weight-at-age data is improved markedly by allowing temperature to impact growth increment, and particularly by allowing the parameters of the von Bertalanffy growth function to vary among years. Annual variation in κ and ℓ_∞ led to the largest reductions in the objective function (Table 1).

The alternative models are able fit the catches almost perfectly, which was expected given the high weight assigned to those data (see Supplementary Fig. 4, left panels for the fits for models 0 and 9) while the models capture the general trend in the survey index (Supplementary Fig. 4, right panels). All models fail to mimic the reduction in survey biomass in 2018 and 2019, as did the actual stock assessment (Supplementary Figs 4 and A.1). The fits of the models to the fishery and survey age-composition exhibit "clumps" of residuals, but the fits to these data do not differ much between models (Supplementary Fig. 5). In contrast to the fits to catch, survey index and age-composition data, the models that allow for annual variation in the parameters of the growth function and temperature effects on growth increment fit the survey weight-at-age data appreciably better than the null model (contrast the fits to these data for models 0 and 9 in Fig. 2).

To reduce the volume of results, the subsequent analyses are based on the null model (0), model 4 (time-varying growth based on time-varying ℓ_∞ but no cold pool extent impact on recruitment), model 5 (cold pool extent impact on recruitment but time-invariant growth), model 6 (cold pool extent impact on recruitment, temperature impact on growth increment and time-invariant growth) and models 8 and 9 (cold pool extent impact on recruitment, temperature impact on growth and annually varying growth function parameters). These models were selected because they included the null model, the models that were

[10] The values for the objective function in Table 1 are directly not comparable because the penalties included in the objective function differ among the models. Moreover, the weights assigned to the index and composition data (Supplementary Appendix A) were taken from the actual assessment and not tuned given the fit of the model to the data while the weights assigned to the weight-at-age data were based on number of animals aged. The latter in particular may overweight the contribution of the weight-at-age data to the objective function if there is clustering in the animals that were aged and weighed (c.f., Pennington and Volstad, 1994). Thus, large differences can be interpreted as real differences in fit, but cannot be used as the basis for formal model comparison.

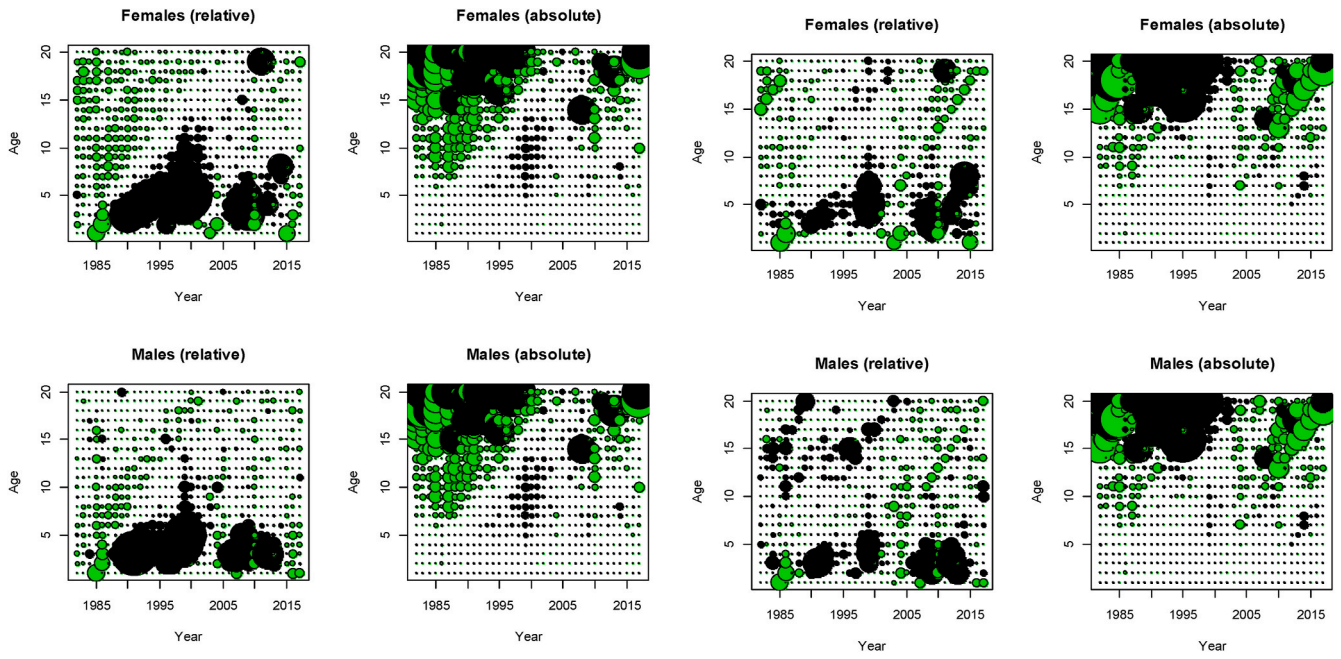

Fig. 2. Fit of the population dynamics model to the survey weight-at-age data for models 0 (no environmental effects; left two columns) and 9 (temperature effect on annual growth increment, annual varying ℓ_∞; cold pool impact on recruitment; right two columns). Results are shown for residuals (positive green; negative black) expressed relative to the expected value ("relative") and the raw residuals.

amongst those that fit the data best, and alternative models that might have been selected had only environmental variables been considered for possible inclusion in the assessment.

3.2. Bayesian posterior distributions

There is no evidence that the MCMC algorithm failed to converge for any of the six models (see the trace plots for the extent of variation in recruitment σ_R, the parameter that determines the relationship between recruitment and the cold pool extent γ_1, the parameter that determines the relationship between annual deviations in the growth increment and temperature η, and the extent of variation in the annual deviations in κ and ℓ_∞ (σ_κ and σ_{ℓ_∞}) for models 0, 5, 8 and 9 (Supplementary Figs 6-8 [11])).

The posterior distributions for γ_1 and η have most of their posterior probability assigned to the sign expected *a priori* based on the hypotheses for how the overlap between the cold pool and the nursery grounds should impact recruitment and how temperature should impact growth increment (Table 3). However, the magnitude of these parameters is quite small. Including the cold pool extent in the function for expected recruitment leads to a lower value for σ_R, indicating that the overlap between the cold pool and the nursery grounds explains some of the variation in recruitment (Table 3). However, the distributions for σ_R suggest that most of the variation in recruitment is due to unknown factors. The posterior distribution for σ_R is markedly updated compared to the prior (Supplementary Fig. 6), although the prior for σ_R (Supplementary Eqn A.13) was not very informative. Accounting for temperature impacts on growth increment in weight leads to better fits to the data in general but does not lead to lesser unexplained variance in recruitment about expected recruitment.

Supplementary Fig. 9 shows the posterior distributions for the time-trajectories of κ and ℓ_∞. The temporal pattern in deviations is similar for κ and ℓ_∞, with lower (and less precise) values prior to the model start year of 1975 (these deviations determine length-at-age at the start of 1975). The values for ℓ_∞ and particularly κ are estimated to have been below their reference values during the 1980s and above these values towards the end of the modelled period.

Table 3
Posterior distributions (medians and 90 % intervals-parenthesis) for key parameters of the assessment model. The values in brackets are the proportions of the posterior of the expected sign for the hypotheses concerned.

Model	γ_1	σ_R	η	σ_κ	σ_{ℓ_∞}
0	–	0.929 (0.780; 1.152)	–	–	–
4	–	0.936 (0.785; 1.161)	0.007 [0.583] (−0.047; 0.058)	–	
5	−0.701 [0.968] (−1.315; −0.063)	0.898 (0.726; 1.119)	–	–	–
6	−0.713 [0.947] (−1.345; 0.004)	0.885 (0.716; 1.094)	0.116 [1.000] (0.076; 0.153)	–	–
8	−0.594 [0.925] (−1.308; 0.113)	0.914 (0.641; 1.138)	0.010 [0.640] (−0.044; 0.062)	0.219 (0.179; 0.264)	–
9	−0.601 [0.919] (−1.310; 0.097)	0.917 (0.736; 1.123)	0.006 [0.576] (−0.046; 0.060)	–	0.162 (0.123; 0.217)

3.2.1. Deterministic and stochastic projections of recruitment and growth

The estimates of reference points and the projections depend on projected recruitment and growth (reference points: expected recruitment; projections: stochastic recruitment). Fig. 3 shows the distributions for recruitment for the six models. Results are shown when unexplained

[11] These are the parameters which took longest to converge.

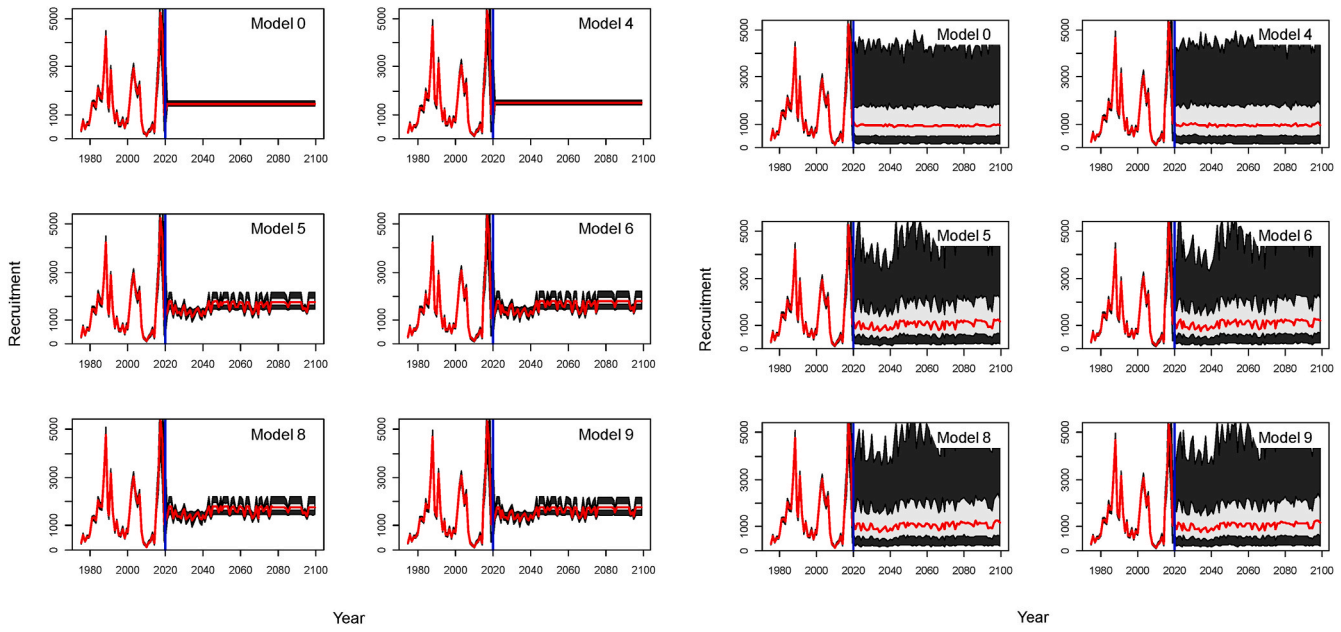

Fig. 3. Posterior distributions (red line median, light shading 50%-iles, dark shading 90%-iles) for recruitment for the six models. The left two columns show deterministic projections based on downscaled GFDL-ESM2M under RCP 8.5 (i.e., $\sigma_R = \sigma_\kappa = \sigma_{\ell_\infty}$) and those in the right two columns when allowance is made for recruitment variation and the variation in the parameters of the growth function. The upper right corners of the distributions in the right panels are truncated after 2060 to allow the captions to be displayed.

variation (quantified through σ_R) is ignored (left two columns) and when σ_R (and hence the deviations in recruitment about its expected value) is sampled from the posterior distribution (right two columns). Future recruitment is independent of time for models 0 and 4, while expected recruitment increases over time for models 5, 6, 8 and 9 (the estimated effects of declining pH being less consequential than the effects of reductions in the cold pool extent; see Eqn (11) for the formulation for how these variables impacted recruitment) (Fig. 3, left two columns). Expected recruitment increases to a maximum for each draw from the posterior because the lowest value for cold pool extent is zero (Supplementary Fig. 1). Including variation in recruitment due to unknown sources swamps the effects of changes over time in cold pool extent and pH (Fig. 3, right two columns). Some of the recruitment estimates are outside the range of the generated values but the distributions generally represent the historical variation in recruitment well, if allowance is made for unknown sources of recruitment variation as well as variation due to cold pool extent (definitely for model 9, almost for model 8).

Fig. 4 shows distributions for the weight-at-age of females of age 8 (a representative age-class) for the six models. Results are shown in the left two columns when annual variation in the parameters of the von Bertalanffy growth function is ignored and when this variation is accounted for in the right two columns. The effect of temperature on the expected growth increment in weight is more evident for model 6 than for models 4, 8 and 9 because the latter three models capture much of the variation in weight-at-age due to variation in the parameters that determine length as a function of age. As expected, accounting for variation in the parameters that determine length-at-age (models 4, 8, and 9) leads to considerable variation in weight-at-age, with the effects of variation in ℓ_∞ (models 4 and 9) having a larger effect on weight-at-age than variation in κ (model 8) (Fig. 4, right panels). Models 0, 5 and 6, which do not include annual variation in parameters of the growth function do not capture the historical variation in weight-at-age.

3.3. Estimates of yield and economic reference points

3.3.1. Estimates in the absence of environmental-related drivers

The 2nd column of Table 4 summarizes the distributions for the nine reference points for the model that has no environmental drivers of recruitment or growth and which ignores annual variation in the parameters of the growth function (model 0). The values for reference points are independent of time for model 0. In addition, $F_{35\%}$ is equal to F_{35} (and $F_{40\%}$ is equal to F_{40}) for model 0 because expected recruitment is time-invariant.

The fishing mortality (and hence effort) corresponding to MSY (Fig. 5a) substantially exceeds the fishing mortality rates observed historically (Supplementary Fig. 10) given that F_{MSY} equals F_{MAX} (fishing mortality rate that achieves maximum yield-per-recruit) in this case because expected recruitment is assumed to be independent of spawning biomass. The high values for F_{MSY} lead to an expected relative biomass $< \sim 10$ % of the unfished level (Table 4; Fig. 5c). This level of depletion is much lower than those at which an Alaskan federally-managed stock would be considered overfished and in need of rebuilding (Anon, 2020) and would not constitute a viable target biomass. The values for F_{MSY} reflect the lack of a stock-recruitment relationship so that the same recruitment is assumed to occur irrespective of the level of spawning biomass. Given this, the remainder of the paper does not comment on the estimates of F_{MSY}, MSY, E_{MSY} and B_{MSY}/B_0

The values for $F_{35\%}$ (F_{35}) and $F_{40\%}$ (F_{40}) are much smaller than those of F_{MSY}, and within the range of fishing mortality rates observed historically (Supplementary Fig. 10). The fishing mortality rate corresponding to maximum economic yield (F_{MEY}) (median 0.058yr^{-1}; 90 % interval 0.052–0.065yr^{-1}) is substantially lower than the other fishing mortality reference points reflecting the trade-off between revenue and cost, which depends on the price/cost ratio (Supplementary Appendix C). The posterior median for effort (in days) at MEY is 577 days (90 % interval 528–642), corresponding to an MEY profit of $17.2 M (90 % interval $13.8–21.7 M) (and catch at MEY of 52,700t; 90 % interval

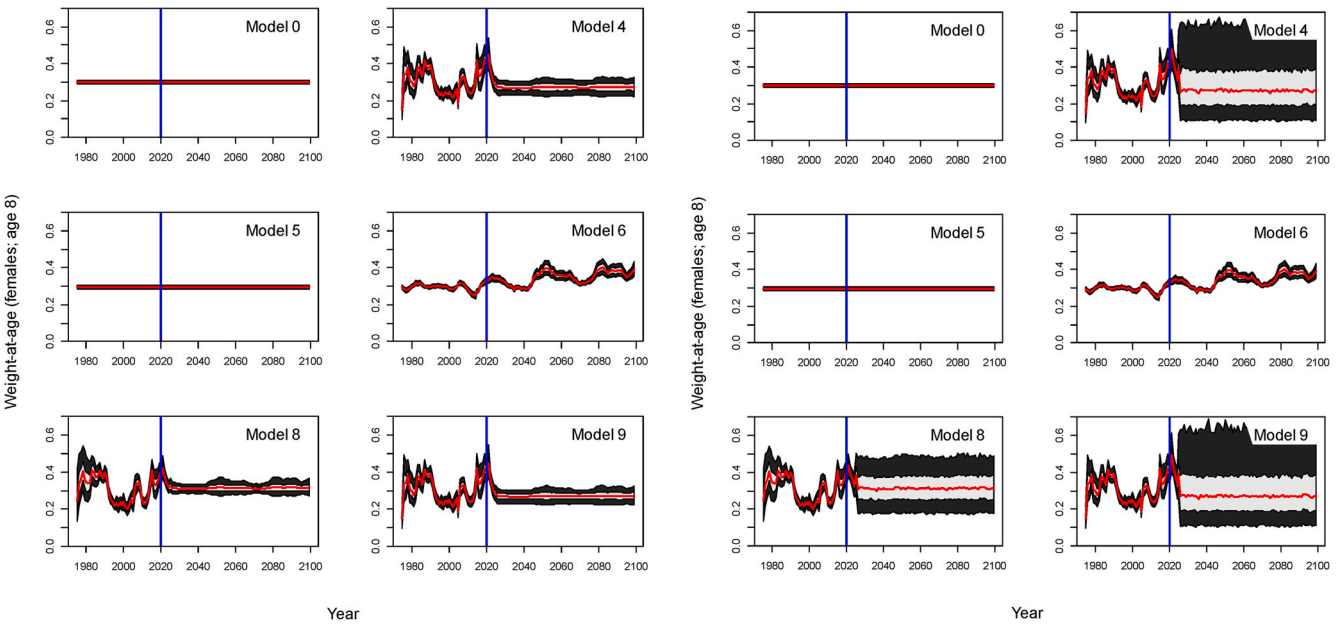

Fig. 4. Posterior distributions (red line median, light shading 50%-iles, dark shading 90%-iles) for the weight of a female of age 8 for the six models. The left two columns show deterministic projections based on downscaled GFDL-ESM2M under RCP 8.5 (i.e., $\sigma_R = \sigma_\kappa = \sigma_{\ell_\infty}$) and those in the right two columns when allowance is made for recruitment variation and the variation in the parameters of the growth function. Note that the distributions for models 4 and 9 are truncated after 2060 to allow the caption to be shown.

Table 4
Values for the reference points for models 0, 8 and 9 in 2020 as a function (for models 8 and 9) for how weight-at-age and recruitment are determined.

Model	0	8				9			
Weight-at-age	Constant	2020	2016–20	2020	2016–20	2020	2016–20	2020	2016–20
Recruitment	Constant	2020	2016–20	Dynamic B_0	Dynamic B_0	2020	2016–20	Dynamic B_0	Dynamic B_0
MSY	114.8 (107; 124.5)	180.4 (144.7; 225.9)	160.6 (138; 189.5)	139.2 (124.9; 160.6)	133.3 (119.8; 152.8)	196.5 (157.6; 251.2)	169.8 (144.5; 201.1)	151.5 (133.1; 176.4)	140.2 (125.2; 162.3)
F_{MSY} (yr^{-1})	0.82 (0.6; 1.06)	1.21 (0.77; 1.88)	1.23 (0.79; 1.77)	1.21 (0.77; 1.88)	1.23 (0.79; 1.77)	1.04 (0.65; 1.65)	1.06 (0.71; 1.56)	1.04 (0.65; 1.65)	1.06 (0.71; 1.56)
B_{MSY}/B_0	0.08 (0.06; 0.11)	0.06 (0.03; 0.09)	0.05 (0.03; 0.08)	0.04 (0.02; 0.08)	0.04 (0.02; 0.07)	0.08 (0.04; 0.14)	0.07 (0.04; 0.11)	0.06 (0.03; 0.12)	0.06 (0.03; 0.09)
$F_{35\%}$ (yr^{-1})	0.19 (0.16; 0.24)	0.2 (0.17; 0.25)	0.2 (0.17; 0.25)	0.2 (0.17; 0.25)	0.2 (0.17; 0.25)	0.2 (0.16; 0.25)	0.2 (0.16; 0.25)	0.2 (0.16; 0.25)	0.2 (0.16; 0.25)
$F_{40\%}$ (yr^{-1})	0.16 (0.13; 0.19)	0.17 (0.14; 0.21)	0.16 (0.14; 0.2)	0.17 (0.14; 0.21)	0.16 (0.14; 0.2)	0.17 (0.14; 0.21)	0.17 (0.14; 0.21)	0.17 (0.14; 0.21)	0.17 (0.14; 0.21)
F_{35} (yr^{-1})	0.19 (0.16; 0.24)	0.21 (0.17; 0.26)	0.18 (0.15; 0.23)	0.15 (0.08; 0.23)	0.14 (0.08; 0.22)	0.26 (0.2; 0.35)	0.22 (0.16; 0.29)	0.19 (0.11; 0.3)	0.17 (0.1; 0.27)
F_{40} (yr^{-1})	0.16 (0.13; 0.19)	0.17 (0.14; 0.22)	0.15 (0.12; 0.19)	0.12 (0.06; 0.2)	0.11 (0.06; 0.18)	0.22 (0.17; 0.3)	0.18 (0.14; 0.24)	0.15 (0.08; 0.26)	0.14 (0.07; 0.23)
F_{MEY} (yr^{-1})	0.06 (0.05; 0.07)	0.09 (0.07; 0.11)	0.08 (0.06; 0.09)	0.06 (0.05; 0.08)	0.06 (0.05; 0.07)	0.1 (0.08; 0.12)	0.08 (0.07; 0.1)	0.07 (0.06; 0.09)	0.07 (0.06; 0.08)
MEY ('000$)	17.2 (13.5; 21.8)	37.9 (21.8; 63.4)	29.6 (20; 43.8)	19.8 (14.1; 29.5)	18 (12.7; 26.7)	47 (28.6; 76)	33.6 (22.8; 50)	25.3 (18.1; 36)	20.8 (14.7; 29.2)
B_{MEY}/B_0	0.7 (0.6; 0.7)	0.6 (0.5; 0.7)	0.6 (0.5; 0.7)	0.5 (0.4; 0.7)	0.5 (0.4; 0.7)	0.7 (0.5; 0.8)	0.6 (0.5; 0.8)	0.6 (0.4; 0.8)	0.6 (0.4; 0.7)
C_{MEY} ('000t)	52.7 (45.8; 60.9)	93.8 (65; 136.6)	78.5 (60.1; 103.1)	60 (48.2; 78.3)	55.8 (45.4; 72.1)	109.4 (77.1; 155.4)	86.4 (66.5; 114.5)	71 (56.8; 90.5)	62 (50.1; 77.8)
E_{MSY} (days)	8150 (5935; 10460)	12466 (7872; 19128)	12601 (8109; 18293)	12466 (7872; 19128)	12602 (8109; 18294)	10669 (6686; 16852)	10848 (7374; 15838)	10669 (6690; 16852)	10849 (7374; 15839)
E_{MEY} (days)	577 (528; 642)	903 (699; 1142)	793 (656; 953)	656 (562; 789)	619 (532; 743)	1007 (787; 1277)	855 (707; 1033)	742 (629; 891)	674 (574; 798)

45,8–60,900t). The intervals given in the 2nd column of Table 4 reflect variation due to fishing at F_{MEY}. The intervals corresponding to fishing at the median value for E_{MEY} (577 days) is appreciably wider (Fig. 5b).

3.4. *Effects of environmental variables*

Figs. 6 and 7 show the distributions for six of the reference points against time for models 8 and 9 (the results for model 4 are qualitatively identical to those for model 9; Supplementary Fig. 11; those for models 5

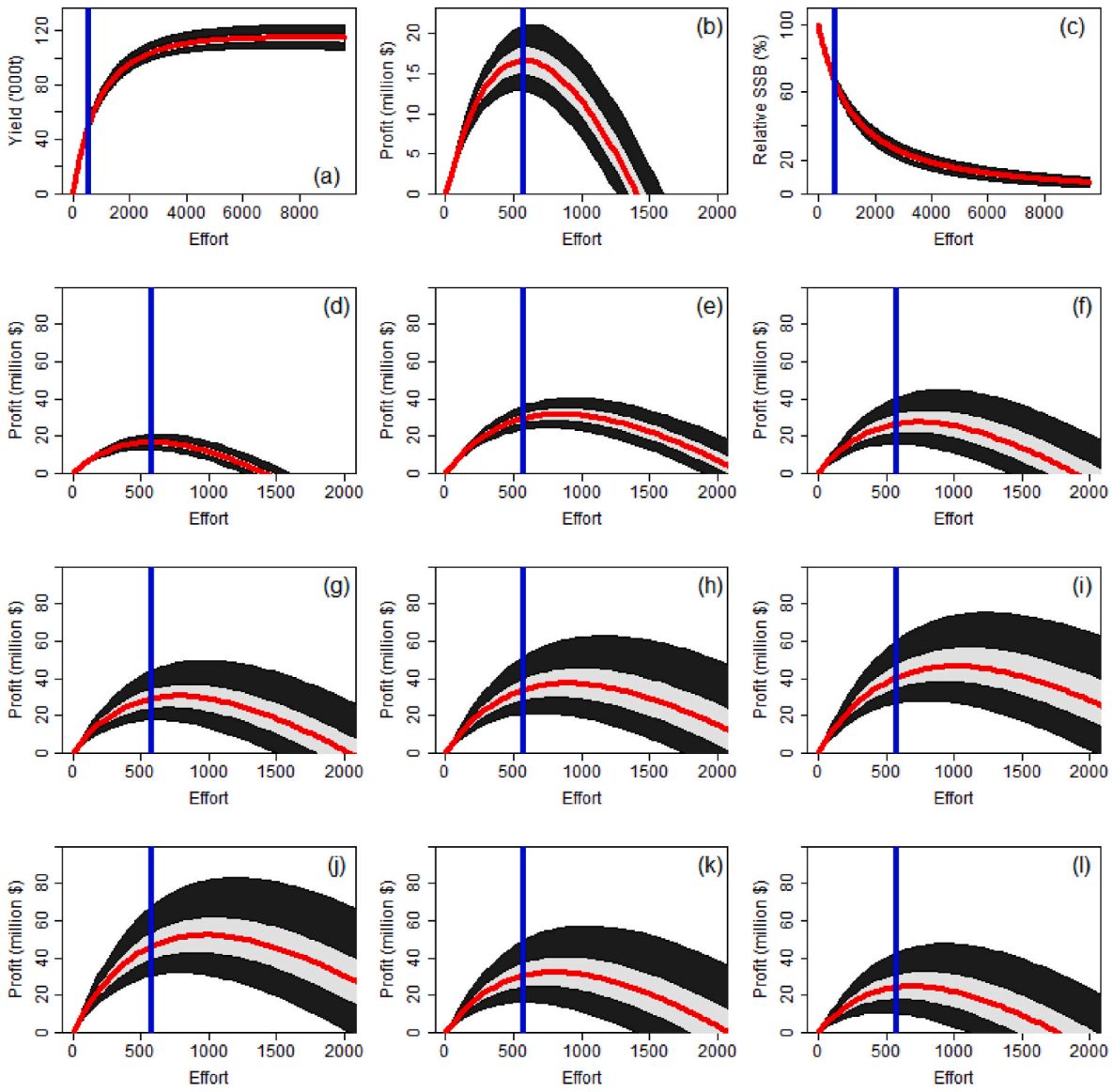

Fig. 5. Relationship between yield, profit and relative reduction in spawning biomass as a function of fishing effort for model 0 (panels a, b, c), the relationship between profit and fishing effort in 2020 for models 0, 4, 5, 6, 8, 9 (Table 2) (panels d–i), and the relationship between profit and fishing effort in 2090 for models, 6, 8, 9 (Table 2) (panels d–i). The results in panels a-i assume the reference values for the growth parameters, the 2016–20 weights-at-age and the "dynamic B_0" approach for setting recruitment. The red line is median of the posterior distribution, the light shading covers 50 % of the posterior, and the dark shading 90 % of the posterior. The vertical line is the median E_{MEY} for model 0.

and 6 exhibit less variability owing to not accounting for changes over time in the growth parameters; Supplementary Figs 12-13). The yield functions for the six models for 2020 are shown in the lower panels of Fig. 5. As expected, there are differences in results due to the way that annual variation in the parameters of the growth function is modelled (green, red and blue box plots in Figs. 6 and 7; Supplementary Fig. 11), as well as due to how expected weight-at-age and relative recruitment are set (dynamic B_0, most recent year, average over the most recent five years). The effects on the values for the reference points of cold pool extent are more marked than those of pH (contrast Supplementary Figs 14 and 12).

The values for the reference points in the first year (2020) are the same for each model because they are based on the same values for recruitment and weight-at-age given the approach for setting weight-at-age and recruitment. The largest effect on the reference points is whether growth is faster (blue box plots) or slower (green box plots) than expected (red box plots), with the effect increasing as the cohorts that are currently in the population die out (i.e., over time). The effect of growth is greatest for the reference points related to maximum economic yield, with F_{MEY} close (or equal to) zero for the slow growth case. In contrast, optimal fishing mortality rates (and effort levels) would be substantially larger were growth to increase to the upper 5%-ile of the estimated distributions for ℓ_∞ or κ. F_{40} is independent of time for the models with time-varying ℓ_∞ because changing ℓ_∞ for each cohort by the same amount leads to a change in weight-at-age that is the same for all age-classes. In contrast, changing κ for each cohort by the same amount leads to changes in weight-at-age that are more marked for the older age-classes.

Although the growth rate is the most influential parameter, the values of the reference points depend on other factors as well. Basing recruitment and weight-at-age on the most recent year leads to higher values for F_{35}, F_{40}, and F_{MEY} (e.g., Table 5), but this is a transient effect. Model 4 leads to higher values for F_{35}, F_{40}, and F_{MEY} and models 5, 6 and 8 to lower values. The values for F_{35} and F_{40} are largely time-invariant given an assumption regarding whether growth is faster or slower than expected. In contrast, quantities such as F_{MEY}, MEY and C_{MEY} differ

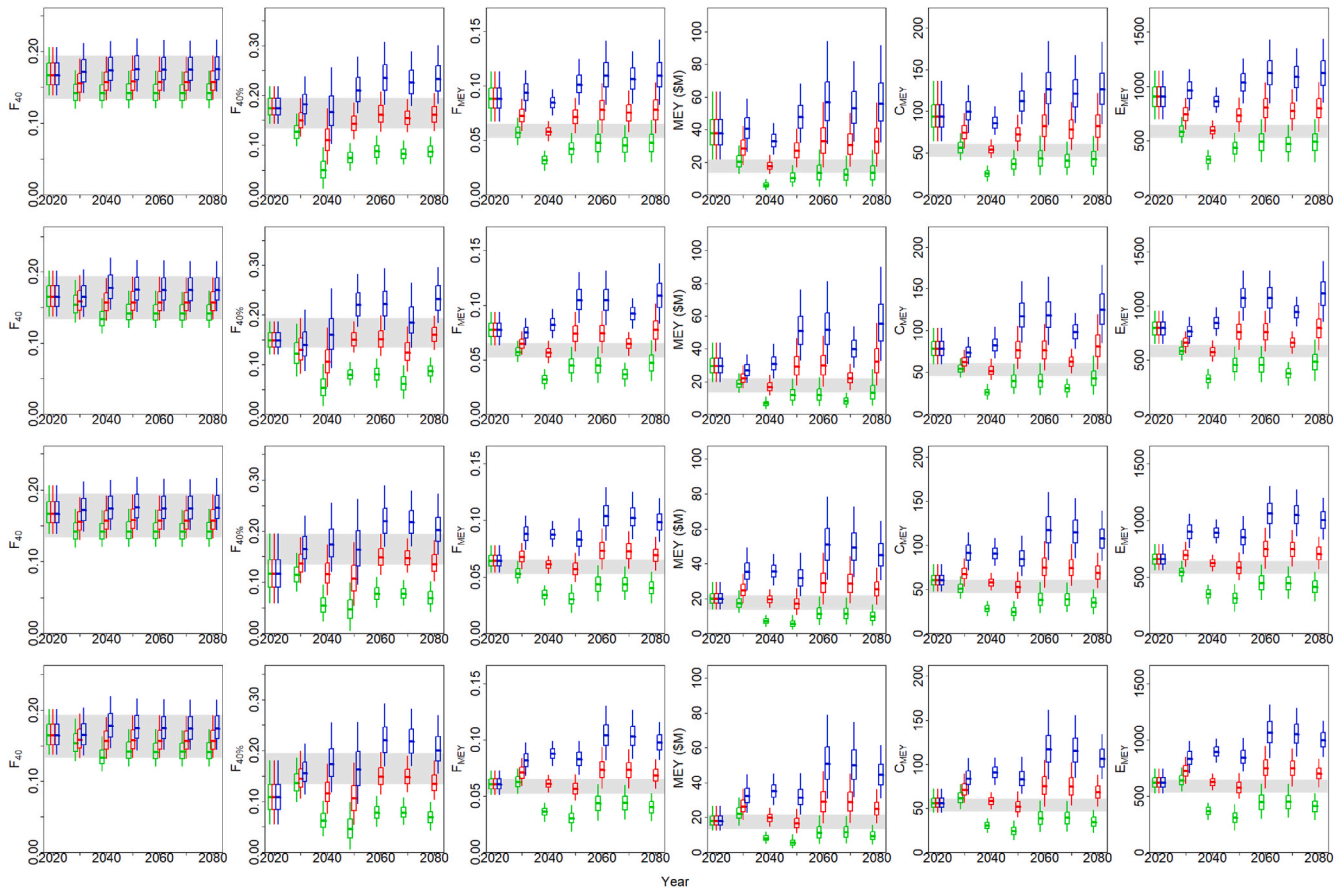

Fig. 6. Distributions (boxes extend to 50 % of the distributions and whiskers to the upper and lower 5%iles) for six reference points for model 8, with results shown for recruitment and weight-at-age based on those for the year concerned (top panels), for the average recruitment and weight-at-age for the five years prior to the year concerned (2nd row of panels), for weight-at-age based on that for the year concerned and dynamic B_0 recruitment (3rd row of panels), and for average weight-at-age for the five years prior to the year concerned and dynamic B_0 recruitment (bottom panels). Results when κ is set to the lower 5%-iles, median and upper 5%-iles are shown in green, red and blue respectively. The horizontal light gray shading indicates the 90 % intervals for model 0. Projections are based on downscaled GFDL-ESM2M under RCP 8.5.

markedly between evaluations in 2020 and 2090 even given the same model and assumptions regarding ℓ_∞ or κ (Table 5; Figs. 6 and 7, Supplementary Figs 11-13). The change in results from 2020 to 2090 is most marked for model 6, which assumes that there is no variation in growth parameters and all of the variation in weight-at-age is due to an effect of temperature on growth increment (Table 5; Supplementary Fig. 13).

3.5. Projections

The probability of spawning biomass dropping below the Minimum Stock Size Threshold (17.5 % of the unfished level) is less than 2 % for all harvest strategies and models on which projections are based. The extent of inter-annual variation in catch is similar for all strategies but lowest for the strategy for which fishing mortality is set to the average over 2016–20 (Supplementary Table 1). Consequently, the focus for this section is the impact of the choice of the harvest strategy on profit (Figs. 8 and 9; see Supplementary Figs 15 and 16 for results for average catch).

Almost all of the strategies lead to distributions for profit during 2020–29 that exceed that corresponding to the average fishing mortality during 2016–20 (Fig. 8), with the benefits of the alternative harvest strategies greatest for model 9 (lower panel) and smallest for model 0 (upper panel). The probability of negative profit in any given year is lowest for model 9 and greatest for model 0, implying that ignoring climate effects results in a more pessimistic outcome for the fishery (assuming model 9 reflects the true situation rather than model 0). The benefits of adopting one of the harvest strategies compared to the average fishing mortality is much less evident for 2090–99, with the strategies based on target reference points of F_{40} and $F_{40\%}$ often leading to very high probabilities of negative profit (often in more than 50 % of years when the projections are based on model 9). In contrast, the strategies based on a target fishing mortality of F_{MEY} achieve equal (or greater) profit than average fishing mortality, but the extent of improvement is generally limited. There is negligible difference in results between the constant fishing mortality and 40-5 harvest strategies primarily because biomass is not often driven below 40 % of unfished spawning biomass. Catches for the strategies based on F_{40} and $F_{40\%}$ are much larger than those based on average fishing mortality or F_{MEY} (Supplementary Figs 15 and 16), but the increased costs associated with those strategies outweigh the additional revenue due to higher catches.

4. Discussion

4.1. The projection methodology

Projections of catch and spawning biomass (and much less frequently profit) are regularly conducted as part of fisheries stock assessments. They are used to form the basis for catch limits and to evaluate the consequences of alternative harvest strategies. The results of projections are often presented as decision tables to allow the effects of different strategies and alternative models to be quantified and contrasted (PFMC, 2020). The types of uncertainties included in projections vary

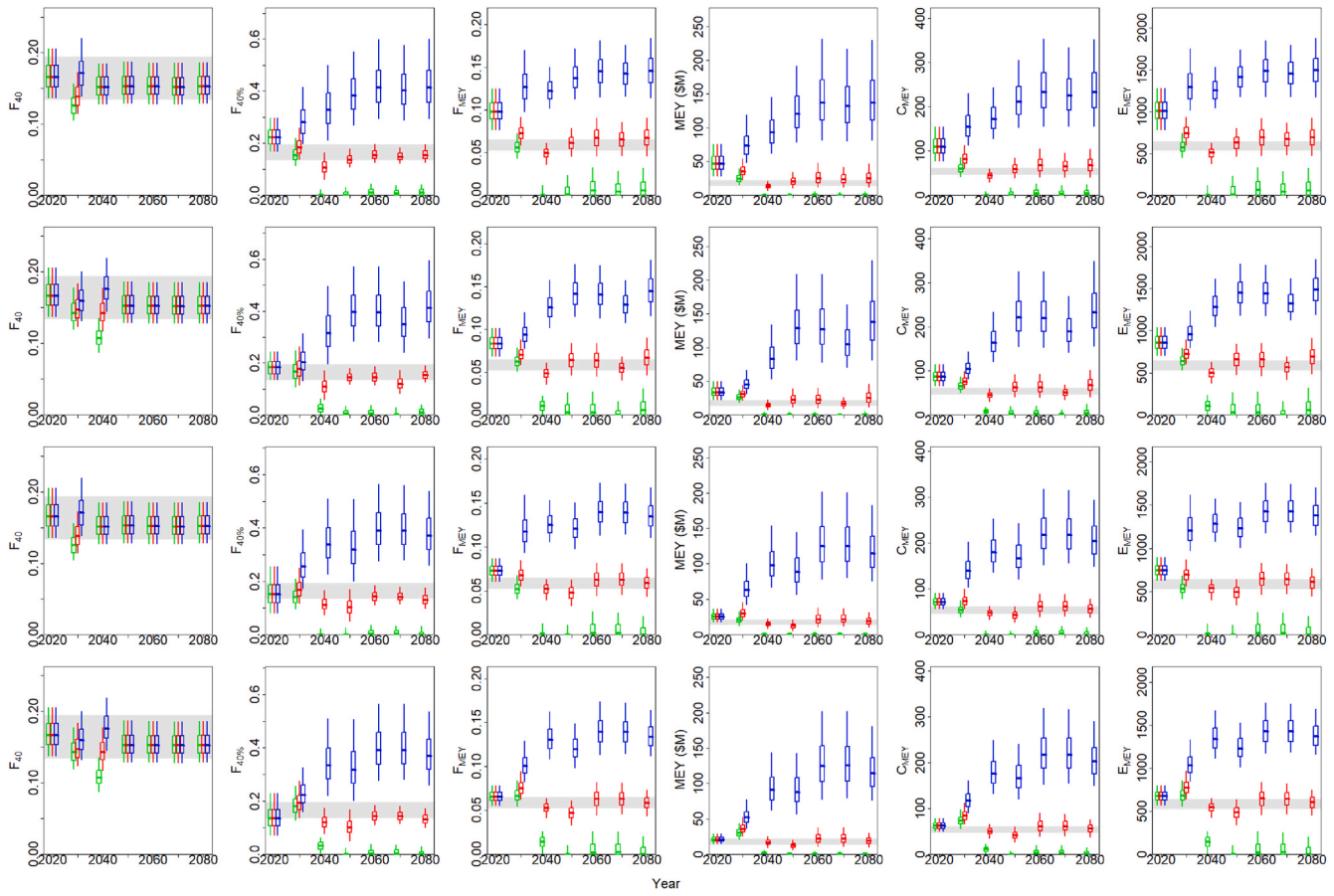

Fig. 7. Distributions (boxes extend to 50 % of the distributions and whiskers to the upper and lower 5%iles) for six reference points for model 9, with results shown for recruitment and weight-at-age based on those for the year concerned (top panels), for the average recruitment and weight-at-age for the five years prior to the year concerned (2nd row of panels), for weight-at-age based on that for the year concerned and dynamic B_0 recruitment (3rd row of panels), and for average weight-at-age for the five years prior to the year concerned and dynamic B_0 recruitment (bottom panels). Results when ℓ_∞ is set to the lower 5%-iles, median and upper 5%-iles are shown in green, red and blue respectively. The horizontal light gray shading indicates the 90 % intervals for model 0. Projections are based on downscaled GFDL-ESM2M under RCP 8.5.

markedly among applications, with the simplest projections based on a single model and no uncertainty quantified. The projections of this paper include several of the sources of uncertainty outlined by Francis and Shotten (1997), each of which was consequential. Specifically:

- model error in the form of whether and how environmental factors (changes over time in pH and temperature) impact growth and expected recruitment;
- process error in recruitment about expected recruitment, and inter-annual variation in the parameters of the von Bertalanffy growth function; and
- observation error, which results in posterior distributions for the parameters of the models.

The projections do not account for implementation error, assuming instead that fishing mortality is implemented as intended by the harvest strategies. One form of implementation error would be whether the catch limits implied by the harvest strategies would be implemented as implied by the calculations of the paper. Almost all (98 %, based on the supplementary data reported in Appendix C) northern rock sole catch occurs in the North Pacific Fishery Management Council Amendment 80 fishery, where this catch comprises a fraction (~17 %) of the combined catch of Amendment 80 species in the Bering Sea (i.e., Atka mackerel, flathead sole, Pacific cod, rock sole, and yellowfin sole) for Amendment 80 vessels with northern rock sole catch. In particular, yellowfin sole accounts for half of their Amendment 80 catch. A source of implementation error could be omitted costs of quota transfers among these vessels; Amendment 80 allows the formation of cooperatives to minimize these costs.

The effects of climate and environmental variation are represented in the modeling in two ways: (a) as offsets to the values of parameters (the 'mechanistic' approach), and (b) as sources of process error (the 'process error approach'). The former approach (adopted for the effects of pH and cold pool extent on recruitment and temperature on growth increment) has the advantage that it is fairly straightforward to conduct projections given the results of downscaled earth system models. However, this approach relies on identification of hypotheses regarding how climate and environmental variation impact demographic processes and the availability of relevant covariates (both historically and in the future). In contrast, capturing the effects of changing climate and environmental variation using process error does not require the development of hypotheses and identification of covariates, rather "letting the data speak for themselves". However, as was the case in this paper, forecasting process error (in recruitment and growth parameters) is not straightforward as there is no mechanism underlying the process error. The uncertainty in growth parameters was captured here by calculating reference points when the growth parameters after 2020 equalled the lower 5%-iles, medians and upper 5%-iles of the estimated distributions, and by conducting projections by sampling these growth parameters from distributions.

The environmental drivers of the demographic parameters are included in the projections in two ways. The first is to fully integrate the

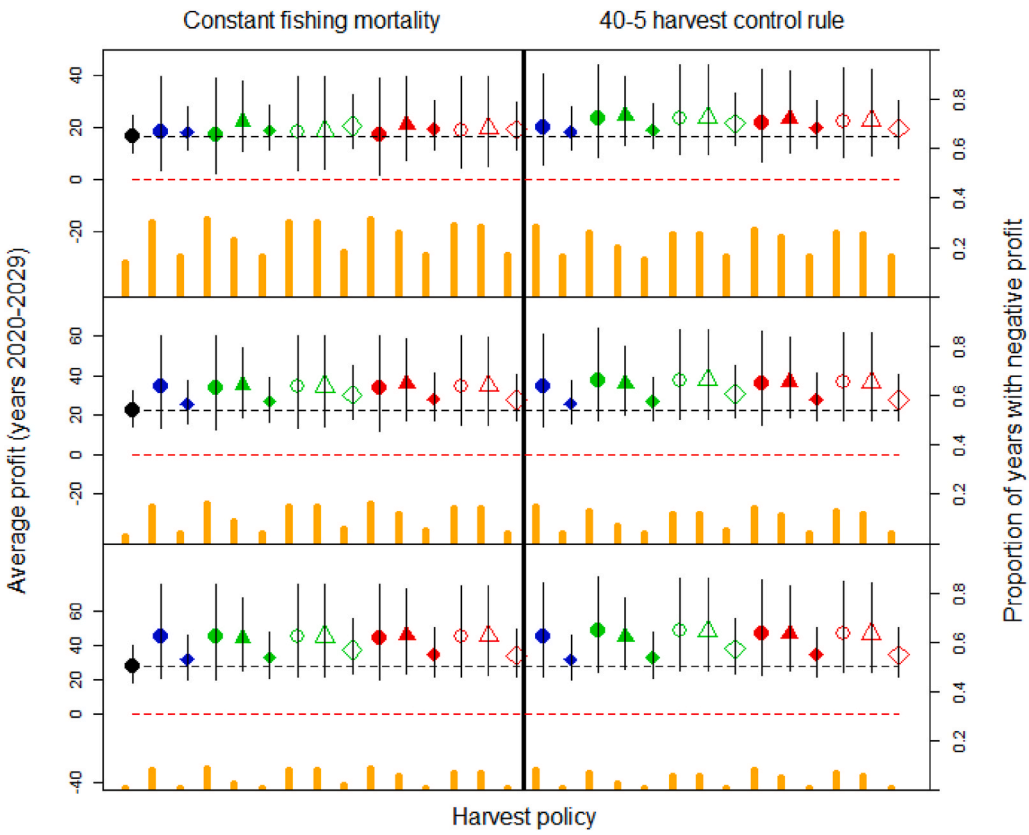

Fig. 8. Average profit (million $) (2020–2029) [median and 90 % intervals] by harvest strategy and the proportion of years with negative profit (orange bars). Results are shown for projections based on model 0 in the upper panel, for model 8 in the centre panel and for model 9 in lower panel. The black symbols refer to the strategy based on average fishing mortality for 2016–20, the blue symbols to strategies based on the null model, the green symbols to the strategies based on model 8, and the red symbols to the strategies based on model 9. The closed symbols refer to reference points calculated for 2020 and the open symbols to those calculated for 2090. The red dashed line represents zero average profits, and the black dashed line denotes the median profit for the strategy based on average fishing mortality for 2016-20 The target fishing mortalities are $F_{35\ \%}$ (circle), F_{35} (triangle), and F_{MEY} (diamond).

Table 5
Values for the reference points for the models based on average weight-at-age for the most recent five years and the dynamic B_0 approach for determining recruitment. Results are shown for model 0 and models 4, 5, 6, 8 and 9 for 2020 and 2090.

		2020					2090				
Model	0	4	5	6	8	9	4	5	6	8	9
$F_{35\%}$	0.19 (0.16; 0.24)	0.2 (0.17; 0.25)	0.19 (0.16; 0.24)	0.19 (0.16; 0.23)	0.2 (0.17; 0.25)	0.2 (0.16; 0.25)	0.19 (0.16; 0.24)	0.18 (0.15; 0.22)	0.19 (0.16; 0.24)	0.19 (0.16; 0.24)	0.19 (0.16; 0.24)
$F_{40\%}$	0.16 (0.13; 0.19)	0.17 (0.14; 0.2)	0.16 (0.13; 0.2)	0.16 (0.13; 0.19)	0.16 (0.14; 0.2)	0.17 (0.14; 0.21)	0.16 (0.13; 0.19)	0.15 (0.13; 0.18)	0.16 (0.13; 0.2)	0.16 (0.13; 0.2)	0.16 (0.13; 0.19)
F_{35}	0.19 (0.16; 0.24)	0.24 (0.18; 0.31)	0.13 (0.08; 0.2)	0.12 (0.07; 0.19)	0.14 (0.08; 0.22)	0.17 (0.1; 0.27)	0.19 (0.16; 0.24)	0.19 (0.15; 0.24)	0.18 (0.15; 0.23)	0.25 (0.2; 0.33)	0.19 (0.15; 0.25)
F_{40}	0.16 (0.13; 0.19)	0.2 (0.15; 0.26)	0.1 (0.06; 0.16)	0.09 (0.05; 0.16)	0.11 (0.06; 0.18)	0.14 (0.07; 0.23)	0.16 (0.13; 0.19)	0.16 (0.12; 0.2)	0.15 (0.13; 0.19)	0.21 (0.17; 0.27)	0.16 (0.12; 0.2)
F_{MEY}	0.06 (0.05; 0.07)	0.07 (0.06; 0.08)	0.05 (0.04; 0.06)	0.05 (0.04; 0.06)	0.06 (0.05; 0.07)	0.07 (0.06; 0.08)	0.06 (0.05; 0.07)	0.06 (0.04; 0.07)	0.07 (0.06; 0.09)	0.1 (0.08; 0.12)	0.08 (0.06; 0.1)
MEY	17.2 (13.5; 21.8)	26.1 (20.1; 33.3)	13.2 (9.6; 18)	13.1 (9.8; 19.1)	18 (12.7; 26.7)	20.8 (14.7; 29.2)	17.2 (13.5; 21.8)	16.5 (8; 27.3)	26.1 (16; 40.6)	49.6 (31.6; 76.6)	31 (16.8; 52.8)
B_{MEY}	0.7 (0.6; 0.7)	0.7 (0.6; 0.8)	0.5 (0.4; 0.7)	0.5 (0.4; 0.6)	0.5 (0.4; 0.7)	0.6 (0.4; 0.7)	0.7 (0.6; 0.7)	0.7 (0.6; 0.8)	0.6 (0.5; 0.7)	0.7 (0.6; 0.8)	0.6 (0.5; 0.7)
C_{MEY}	52.7 (45.8; 60.9)	72.6 (61.1; 85.4)	44.3 (36.6; 54.2)	43.8 (36.5; 55.8)	55.8 (45.4; 72.1)	62 (50.1; 77.8)	52.7 (45.8; 60.9)	51 (32; 71.5)	69.7 (50.9; 94.7)	109.2 (80.6; 149.5)	78.9 (52; 115.6)
E_{MEY}	577 (528; 642)	753 (668; 853)	508 (443; 591)	503 (441; 600)	619 (532; 743)	674 (574; 798)	577 (528; 642)	565 (397; 717)	711 (571; 870)	956 (782; 1165)	774 (578; 1000)

associated covariates into the stock assessment (in the case of northern rock sole, cold pool extent and temperature) and the second is to estimate the impact of the drivers on demographic parameters outside of the assessment (in the case of northern rock sole, pH). The first approach, although computationally more intensive, is preferrable because (in principle) the drivers can impact the estimates of demographic parameters and hence historical abundance. In the case of northern rock sole, the estimates of weight-at-age differed depending on whether a

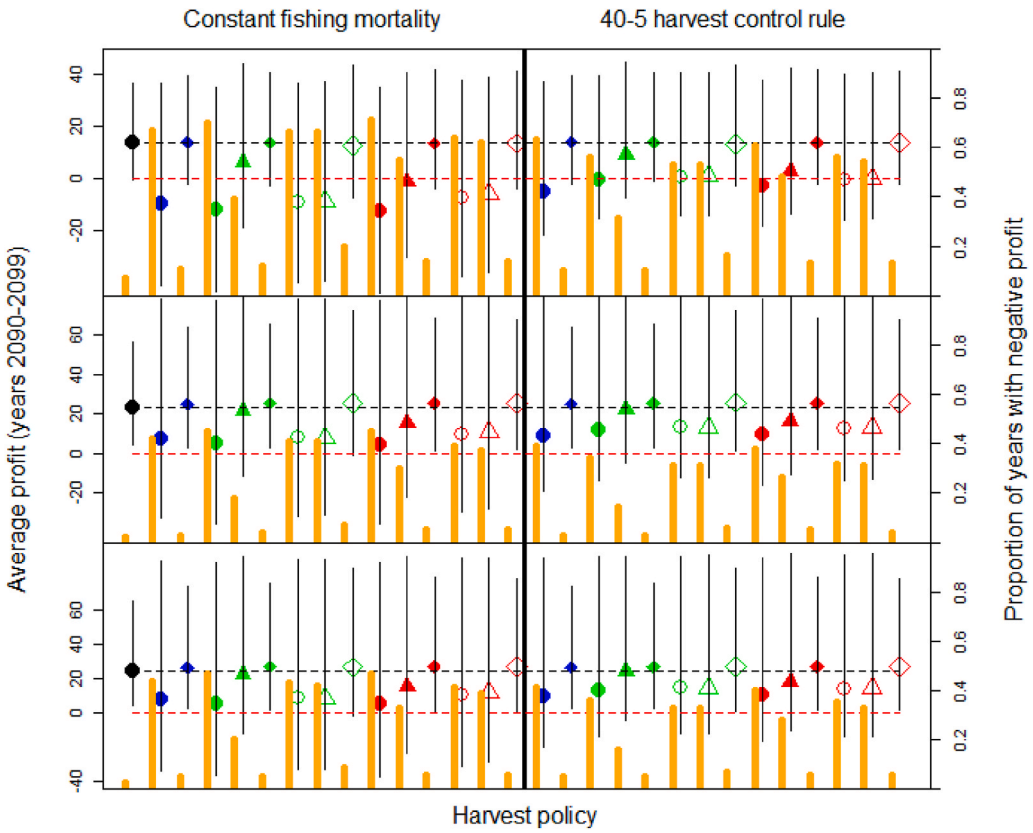

Fig. 9. As for Fig. 8, except the results pertain to 2090-99 based on downscaled GFDL-ESM2M under RCP 8.5.

temperature impact on growth increment was included in the assessment and the estimate of the extent of variation in recruitment was (slightly) lower when allowance was made for an impact of cold pool extent on expected recruitment.

The framework of this paper calculated economic reference points that maximize estimated profits of the rock sole fishery in the Bering Sea. The calculation of economic reference points that account for prices and costs provides information that can be used when setting Total Allowable Catches, which need to be less than or equal to the Acceptable Biological Catch (set for most Alaskan groundfish using the 40-5 harvest strategy with a target fishing mortality of $F_{40\%}$).

4.2. Application of northern rock sole

All of the models led to fits comparable to those of the assessment on which management advice is currently based, and there was no evidence that the MCMC algorithm failed to converge for the models examined. The fits of the extended stock assessment are, however, not ideal given the residual patterns for the age composition and weight-at-age data and the lack of fit to the index during recent years, although the actual assessment also has very similar issues. The extended assessment, in common with the actual assessment leads to some high early estimates of fishing mortality, and to ensure comparability with the existing stock assessment, no attempt was made to tune the data weights. These aspects should be addressed if the extended stock assessment was planned to replace the current assessment, but this was done here to ensure comparability with the existing stock assessment. Unlike most Bayesian stock assessments, it was possible to derive posterior distributions for the extent of variation in recruitment about its expected value and the parameters that quantify inter-annual variation in ℓ_∞ and κ.

The application to northern rock sole indicated support for the hypotheses related to how recruitment and growth increment are related to the environmental drivers, but the quantitative effects of these drivers on reference points and projections were much smaller than those projected by Punt et al. (2014, 2016, 2020) for Alaskan crab stocks. The covariates used to represent the hypotheses explained a relatively small proportion of the variance in recruitment and growth, indicating that (currently) unknown factors are the primary drivers of variation in these demographic parameters. Thus, while leading to better fits to the data, these environmental drivers of recruitment and growth may not have substantial demographic effects. This is one reason that estimates of historical biomass are generally insensitive to inclusion of environmental factors (e.g., Supplementary Figs A.1 and A.2).

The values of the reference points are somewhat sensitive to model choice with model 4 leading to higher values for F_{35}, F_{40}, and F_{MEY} and models 5, 6 and 8 to lower values. Thus, whether and how environmental factors are included in models is consequential for management advice. Most previous attempts to integrate environmental variables into stock assessments have used either the mechanistic or process approaches but seldom both – this study suggests support for both types of approaches, as well as including relationships between demographic parameters and environmental variables developed outside the assessment (even though this not ideal).

Acceptable Biological Catches for northern rock sole are based on the 40-5 strategy with a $F_{40\%}$ target fishing mortality. However, the projections suggest that lower target fishing mortality (closer to those during 2016–20) will lead to greater profit but also to lower yields.

4.3. Future work and caveats

The framework of this paper allows climate and environmental factors to be integrated into stock assessments, calculation of reference points and projections. However, there are several areas for future work. For example, the hypotheses that led to the drivers of expected recruitment and growth increment were based on past work (and for pH experimental results). However, there are many other potential drivers of

population demographics (e.g., the impact of a changing environment on rates of natural mortality, which could be modelled within the context of multispecies assessment models, e.g. Holsman et al., [2016]). Time-varying natural mortality could be included (if appropriate covariates were available) in the population dynamics model, for example following the approach of Barbeaux et al. (2020). That said, reliance on past studies indicating relationships between environmental covariates and demographic parameters could lead to non-significant effects when assessments are updated given the well-known issue that such relationships often "disappear" over time (Myers, 1998), indicating that either the relationships are non-stationary or were incorrectly identified. Moreover, care needs to be taken to avoid spurious correlations (see, for example, the approaches of Haltuch et al., 2020, who assessed the impact of environmental drivers on recruitment of petrale sole, *Eopsetta jordani*).

The analyses rely on covariates that can be computed from past monitoring information and projected using downscaled climate models. This restricts the set of covariates and induces a 'mismatch' between underlying hypotheses and how they are included in the population dynamics model. In principle, rather than including the covariates directly into relationships such as Eqns (7) and (10), the drivers of demographic parameters could be modelled as random effects (latent variables) that are related (with error) to the measured covariates (e.g., Crone et al., 2019; Schirripa et al., 2009). This approach can more appropriately deal with situations in which values for some covariates are missing for some years and provides a bridge between the mechanistic and process error approaches for including climate and environmental drivers in population dynamics models.

There is confounding between inter-annual variation in growth parameters and temperature-dependent variation in growth increment, with the model selection criteria providing more support for the latter than the former. If independent information was available on the temperature-growth increment relationship (e.g., from experimental results such as is the case for pH), it could be included in the analysis by imposing an informative prior on the parameter ν_2. Similarly, had hindcasts of pH been available for the entire period considered in the assessment, we could have treated the results from the analyses of the experimental data (Supplementary Appendix B) as prior information.

The calculation of reference points and the projections are based on the assumption of constant costs and prices, which can be a reason for predicted negative profits. Northern rock sole is primarily an export commodity, and import demand for northern rock sole can be estimated from US trade data in future work.

The assessment assumed that recruitment was independent of spawning biomass (attempts to estimate a stock-recruitment relationship led to a failure of the MCMC algorithm to converge),[12] but this should be re-examined with additional data given that assuming recruitment is independent of spawning biomass will lead to optimistic results in terms of target levels of fishing mortality and yield/profit. The level of optimism will be largest for strategies that imply lower levels of spawning biomass – the reason little focus was placed on the estimates of F_{MSY} and MSY in this paper. In contrast, results for strategies that imply lower levels of fishing mortality (e.g., those that aim to maximize profit) are likely to be more robust to the assumption that recruitment is independent of spawning biomass. The projections assumed that the deviations in recruitment about expected recruitment (which are determined given the effects of cold pool and pH) are temporally independent and this same assumption is made for future values for ℓ_∞ or κ. There is evidence for serial correlation in the estimates for ℓ_∞ and κ (Supplementary Fig. 10) and future work could consider modeling this serial correlation (e.g., following the approach developed by Johnson et al., [2016]).

[12] A stock-recruitment relationship is used to estimate F_{MSY} and future ABCs for actual management northern rock sole but the fitting of this relationship occurs outside of the model fitting process so is not considered here.

Results are shown by model, although each model is fitted to the same data and it could have been possible to combine results over models by computing model weights (e.g., based on DIC [Spiegelhalter et al., 2002] or WAIC [Watanabe, 2013]). This would have led to most (if not all) of the weight being assigned to model 9 given its (statistically) much better fit to the data (Table 1). Such a weighting approach relies on the weights assigned to each component of the likelihood function being correct, which is unlikely to be the case.

The projection analyses of temperature, cold pool extent, and pH are based on downscaled environmental variables derived from a single simulation of one earth system model under a high-emissions scenario (i.e., GFDL-ESM2M under RCP 8.5). However, it is well known that uncertainty in long-term projections derives from several sources, including intrinsic variability, inter-model structural uncertainty, and alternative emissions scenarios (A'mar et al., 2009; Hawkins and Sutton, 2009; Frölicher et al., 2016; Hollowed et al., 2020; Holsman et al., 2020). Many chemical and physical properties such as pH and temperature can be sensitive to carbon emissions assumptions, while biologically-relevant variables are often dominated by uncertainty related to the structure of model equations and their ability to capture observation-poor processes (Frölicher et al., 2016).

5. Conclusion

A framework is developed that can integrate multiple climate and environmental drivers within a stock assessment, while simultaneously accounting for process error in demographic parameters. Estimates of historical biomass, recruitment and fishing mortality are not markedly impacted for the case study species, northern rock sole, but estimates of target and limit reference points (economic and biological) are sensitive to whether and how environmental factors are included in stock assessments and projections. The general framework of the paper can be applied to data-rich stocks with quantitative stock assessments and hypothesized relationships between environmental variables and demographic parameters.

CRediT authorship contribution statement

André E. Punt: Conceptualization, Formal analysis, Investigation, Writing – original draft, Writing – review & editing, Project administration. **Michael G. Dalton:** Conceptualization, Formal analysis, Writing – review & editing. **Wei Cheng:** Data curation. **Albert J. Hermann:** Data curation. **Kirstin K. Holsman:** Writing – review & editing. **Thomas P. Hurst:** Investigation, Writing – review & editing. **James N. Ianelli:** Investigation, Software, Writing – review & editing. **Kelly A. Kearney:** Data curation. **Carey R. McGilliard:** Conceptualization. **Darren J. Pilcher:** Data curation. **Matthieu Véron:** Software.

Declaration of competing interest

The authors declare that they have no known competing financial interests or personal relationships that could have appeared to influence the work reported in this paper.

Acknowledgements

Robert (Bob) Foy is thanked for providing the original suggestion for this work. Anne Hollowed, Cody Szuwalski, William (Buck) Stockhausen, Martin Dorn (all AFSC) and two anonymous reviewers are thanked for their comments and input on an earlier version of the paper. AEP was supported by NOAA through the NOAA Ocean Acidification Program. This publication is partially funded by the Joint Institute for the Study of the Atmosphere and Ocean (JISAO) under NOAA Cooperative Agreement NA15OAR4320063, Contribution No 2020–1131. This is PMEL contribution number 5230 and EcoFOCI contribution number EcoFOCI-1002.

Appendix A. Supplementary data

Supplementary data to this article can be found online at https://doi.org/10.1016/j.dsr2.2021.104951.

References

A'mar, Z.T., Punt, A.E., Dorn, M.W., 2009. The evaluation of management strategies for the Gulf of Alaska walleye pollock under climate change. ICES J. Mar. Sci. 66, 1614–1632.

Anon, 2020. Stock assessment and fishery evaluation for the groundfish resources of the Bering sea/aleutian islands region. https://apps-afsc.fisheries.noaa.gov/refm/docs/2020/BSAIintro.pdf.

Barbeaux, S., Ferris, B., Palsson, W., Shotwell, K., Spies, I., Wang, M., Zador, S., 2020. Chapter 2: assessment of the pacific cod stock in the gulf of Alaska. https://apps-afsc.fisheries.noaa.gov/refm/docs/2020/GOApcod.pdf.

Barbeaux, S.J., Holsman, K., Zador, S., 2020a. Marine heatwave stress test of ecosystem-based fisheries management in the gulf of Alaska pacific cod fishery. Front. Mar. Sci. 7, 1–21.

Breitburg, D., Levin, L.A., Oschlies, A., Grégoire, M., Chavez, F.P., Conley, D.J., Garçon, V., Gilbert, D., Gutiérrez, D., Isensee, K., Jacinto, G.S., Limburg, K.E., Montes, I., Naqvi, S.W.A., Pitcher, G.C., Rabalais, N.N., Roman, M.R., Rose, K.A., Seibel, B.A., Telszewski, M., Yasuhara, M., Zhangj, J., 2018. Declining oxygen in the global ocean and coastal waters. Science 359, eaam7240. https://doi.org/10.1126/science.aam7240.

Carroll, G., Holsman, K.K., Brodie, S., Thorson, J.T., Hazen, E.L., Bograd, S.J., Haltuch, M.A., Kotwicki, S., Samhouri, J., Spencer, P., Willis-Norton, E., Selden, R.L., 2019. A review of methods for quantifying spatial predator–prey overlap. Global Ecol. Biogeogr. 28, 561–1577.

Claret, M., Galbraith, E.D., Palter, J.B., Bianchi, D., Fennel, K., Gilbert, D., Dunne, J.P., 2018. Rapid coastal deoxygenation due to ocean circulation shift in the northwest Atlantic. Nat. Clim. Change 8, 868–872.

Colt, S.G., Knapp, G.P., 2016. Economic effects of an ocean acidification catastrophe. Am. Econ. Rev. 106, 615–619.

Cooley, S.R., Rheuban, J.E., Hart, D.R., Luu, V., Hare, J.A., Doney, S.C., 2015. An integrated assessment model for helping the United States sea scallop (*Placopecten magellanicus*) fishery plan ahead for ocean acidification and warming. PloS One 10, e0124145. https://doi.org/10.1371/journal.pone.0124145.

Cooper, D.W., Duffy-Anderson, J.T., Norcross, B.L., Holladay, B.A., Stabeno, P.J., 2014. Nursery areas of juvenile northern rock sole (*Lepidopsetta polyxystra*) in the eastern Bering sea in relation to hydrography and thermal regimes. ICES J. Mar. Sci. 71, 1683–1695. https://doi.org/10.1093/icesjms/fst210.

Cooper, D., Rogers, L.A., Wilderbuer, T., 2019. Environmentally driven forecasts of northern rock sole (*Lepidopsetta polyxystra*) recruitment in the eastern Bering Sea. Fish. Oceanogr. 29, 111–121.

Crone, P.R., Maunder, M.N., Lee, H., Piner, K.R., 2019. Good practices for including environmental data to inform spawner-recruit dynamics in integrated stock assessments: small pelagic species case study. Fish. Res. 217, 122–132.

Dahlke, F., Wohlrab, S., Butzin, M., Pörtner, H., 2020. Thermal bottlenecks in the lifecycle define climate vulnerability of fish. Science 369 (6499), 65–70.

Deutsch, C., Ferrel, A., Seibel, B., Portner, H.-O., Huey, R., 2015. Climate change tightens a metabolic constraint on marine habitats. Science 348, 1132–1136.

Dichmont, C.M., Pascoe, S., Kompas, T., Punt, A.E., 2010. On implementing maximum economic yield in commercial fisheries. Proc. Natl. Acad. Sci. Unit. States Am. 107, 16–21.

Dunne, J.P., John, J.G., Shevliakova, E., Stouffer, R.J., Krasting, J.P., Malyshev, S.L., Milly, P.C.D., Sentman, L.T., Adcroft, A.J., Cooke, W., Dunne, K.A., Griffies, S.M., Hallberg, R.W., Harrison, M.J., Levy, H., Wittenberg, A.T., Phillips, P.J., Zadeh, N., 2013. GFDL's ESM 2 global coupled climate-carbon Earth system models. Part II: carbon system formulation and baseline simulation characteristics. J. Clim. 26, 2247–2267.

Fisher, M.C., Moore, S.K., Jardine, S.L., Watson, J.R., Samhouri, J.F., 2021. Climate shock effects and mediation in fisheries. Pro. Nat. Acad. Sci. US. 118, 1–8.

Fournier, D.A., Skaug, H.J., Ancheta, J., Ianelli, J., Magnusson, A., Maunder, M.N., Nielsen, A., Sibert, J., 2012. AD Model Builder: using automatic differentiation for statistical inference of highly parameterized complex nonlinear models. Optim. Methods Software 27, 1–17.

Francis, R.I.C.C., Shotton, R., 1997. "Risk" in fisheries management: a review. Can. J. Fish. Aquat. Sci. 54, 1699–1715.

Frölicher, T.L., Fischer, E.M., Gruber, N., 2018. Marine heatwaves under global warming. Nature 560, 360–364.

Frölicher, T.L., Rodgers, K., Stock, C.A., Cheung, W.W.L., 2016. Sources of uncertainties in 21st century projections of potential ocean ecosystem stressors. Global Biogeochem. Cycles 30, 1224–1243.

Haltuch, M.A., Tolimieri, N., Lee, Q., Jacox, M.G., 2020. Oceanographic drivers of petrale sole recruitment in the California Current Ecosystem. Fish. Oceanogr. 29, 12–136.

Hawkins, E., Sutton, R., 2009. The potential to narrow uncertainty in regional climate predictions. Bull. Am. Meteorol. Soc. 90, 1095–1107.

Hermann, A.J., Gibson, G.A., Bond, N.A., Curchitser, E.N., Hedstrom, K., Cheng, W., Wang, M., Cokelet, E.D., Stabeno, P.J., Aydin, K., 2016. Projected future biophysical states of the Bering Sea. Deep Sea Res. II 134, 30–47.

Hermann, A.J., Gibson, G.A., Cheng, W., Ortiz, I., Aydin, K., Wang, M., Hollowed, A.B., Holsman, K.K., Sathyendranath, S., 2019. Projected biophysical conditions of the Bering Sea to 2100 under multiple emission scenarios. ICES J. Mar. Sci. 76, 1280–1304.

Hollowed, A.B., Holsman, K.K., Haynie, A.C., Hermann, A.J., Punt, A.E., Aydin, K., Ianelli, J.N., Kasperski, S., Cheng, W., Faig, A., Kearney, K.A., Reum, J.C.P., Spencer, P., Spies, I., Stockhausen, W., Szuwalski, C.S., Whitehouse, G.A., Wilderbuer, T.K., 2020. Integrated modeling to evaluate climate change impacts on coupled social-ecological systems in Alaska. Front. Mar. Sci. 6, 775.

Holsman, K.K., Hazen, E.L., Haynie, A., Gourguet, S., Hollowed, A., Bograd, S.J., Samhouri, J.F., Aydin, K., 2019. Towards climate resiliency in fisheries management. ICES J. Mar. Sci. 76, 1368–1378.

Holsman, K.K., Ianelli, J., Aydin, K., Punt, A.E., Moffit, E.A., 2016. Comparative biological reference points estimated from temperature-specific multispecies and single species stock assessment models. Deep Sea Res. II 134, 360–378.

Holsman, K., Haynie, A., Hollowed, A., Reum, J., Aydin, K., Hermann, A., Cheng, W., Faig, A., Ianelli, J.N., Kearney, K., Punt, A.E., 2020. Ecosystem-based fisheries management forestalls climate-driven decline. Nat Comm 11, 4579.

Howard, E.M., Penn, J.L., Frenzel, H., Seibel, B.A., Bianchi, D., Renault, L., Kessouri, F., Sutula, M.A., McWilliams, J.C., Deutsch, C., 2020. Climate-driven aerobic habitat loss in the California Current System. Sci. Adv. 6, 1–12.

Huntington, H.P., Danielson, S.L., Wiese, F.K., Baker, M., Boveng, P., Citta, J.J., De Robertis, A., Dickson, D.M.S., Farley, E., George, J.C., Iken, K., Kimmel, D.G., Kuletz, K., Ladd, C., Levine, R., Quakenbush, L., Stabeno, P., Stafford, K.M., Stockwell, D., Wilson, C., 2020. Evidence suggests potential transformation of the Pacific Arctic ecosystem is underway. Nat. Clim. Change 10, 342–348.

Hurst, T.P., Abookire, A.A., 2006. Temporal and spatial variation in potential and realized growth rates of age-0 northern rock sole. J. Fish. Biol. 68, 905–919.

Hurst, T.P., Laurel, B.J., Hanneman, E., Haines, S.A., Ottmar, M.L., 2017. Elevated CO_2 does not exacerbate nutritional stress in larvae of a Pacific flatfish. Fish. Oceanogr. 26, 336–349.

Hurst, T.P., Laurel, B.J., Mathis, J.T., Tobosa, L.R., 2016. Effects of elevated CO2 levels on eggs and larvae of a North Pacific flatfish. ICES J. Mar. Sci. 73, 981–990.

Ianelli, J.N., Hollowed, A.B., Haynie, A.C., Mueter, F.J., Bond, N.A., 2011. Evaluating management strategies for eastern Bering Sea walleye pollock (*Theragra chalcogramma*) in a changing environment. ICES J. Mar. Sci. 68, 1297–1304.

IPCC, 2019. In: Pörtner, H.-O., Roberts, D.C., Masson-Delmotte, V., Zhai, P., Tignor, M., Poloczanska, E., Mintenbeck, K., Alegría, A., Nicolai, M., Okem, A., Petzold, J., Rama, B., Weyer, N.M. (Eds.), IPCC Special Report on the Ocean and Cryosphere in a Changing Climate. https://www.ipcc.ch/srocc/.

Johnson, K., Councill, E., Thorson, J.T., Brooke, E., Methot, R.D., Punt, A.E., 2016. Can autocorrelated recruitment be estimated using integrated assessment models and how does it affect population forecasts? Fish. Res. 183, 222–232.

Jones, M.C., Berkelhammer, M., Keller, K.J., Yoshimura, K., Wooller, M.J., 2020. High sensitivity of Bering Sea winter sea ice to winter insolation and carbon dioxide over the last 5500 years. Sci. Adv. 6, 1–10.

Kaplan, I.C., Levin, P.S., Burden, M., Fulton, E.A., 2010. Fishing catch shares in the face of global change: a framework for integrating cumulative impacts and single species management. Can. J. Fish. Aquat. Sci. 67, 1968–1982.

Karp, M.A., Peterson, J.O., Lynch, P.D., Griffis, R.B., Adams, C.F., Arnold, W.S., Barnett, L.A.K., DeReynier, Y., DiCosimo, J., Fenske, K.H., Gaichas, S.K., Hollowed, A., Holsman, K., Karnauskas, M., Kobayashi, D., Leising, A., Manderson, J.P., McClure, M., Morrison, W.E., Schnettler, E., Thompson, A., Thorson, J.T., Walter, J.F., Yau, A.J., Methot, R.D., Link, J.S., 2019. Accounting for shifting distributions and changing productivity in the development of scientific advice for fishery management. ICES J. Mar. Sci. 76, 1305–1315.

Kearney, K.A., 2021. Temperature data from the eastern Bering Sea continental shelf bottom trawl survey as used for hydrodynamic model validation and comparison. In: NOAA Tech Memo NMFS-AFSC-415, p. 40p. https://repository.library.noaa.gov/view/noaa/28763.

Kearney, K., Hermann, A., Cheng, W., Ortiz, I., Aydin, K., 2020. A coupled pelagic-benthic-sympagic biogeochemical model for the Bering Sea: documentation and validation of the BESTNPZ model (v2019.08.23) within a high-resolution regional ocean model. Geosci. Model Dev. (GMD) 13, 597–650.

Lanksbury, J., Duffy-Anderson, J., Mier, K., Busby, M., Stabeno, P., 2007. Distribution and transport patterns of northern rock sole, *Lepidopsetta polyxystra*, larvae in the southeastern Bering Sea. Prog. Oceanogr. 72, 39–62.

Lefebvre, K., Quakenbush, L., Frame, E., Huntington, K.B., Sheffield, G., Stimmelmayr, R., Bryan, A., Kendrick, P., Ziel, H., Goldstein, T., Snyder, J.A., Gelatt, T., Gulland, F., Dickerson, B., Gill, V., 2016. Prevalence of algal toxins in Alaskan marine mammals foraging in a changing arctic and subarctic environment. Harmful Algae 55, 13–24.

Lewis, E.R., Wallace, D.W.R., 1998. Program Developed for CO_2 system calculations. Rep. *BNL-61827*. Oak ridge, TN: U.S. Dep. Of energy, oak ridge natl. Lab., carbon dioxide inf. Anal. Cent.

Litzow, M.A., Ciannelli, L., Puerta, P., Wettstein, J.J., Rykaczewski, R.R., Opiekun, M., 2018. Non-stationary climate-salmon relationships in the Gulf of Alaska. Proceed. Roy. Soc. B 285, 2018855. https://doi.org/10.1098/rspb.2018.1855.

Laufkötter, C., Zscheischler, J., Frölicher, T.L., 2020. High-impact marine heatwaves attributable to human-induced global warming. Science 369, 1621–1625.

Matta, M.E., Black, B.A., Wilderbuer, T.K., 2010. Climate-driven synchrony in otolith growth-increment chronologies for three Bering Sea flatfish species. Mar. Ecol. Prog. Ser. 413, 137–145.

McGilliard, C.R., Ianelli, J., Punt, A.E., Wilderbuer, T., Nichol, D., Haehn, R., 2020. Assessment of the northern rock sole in the Bering sea and aleutian islands. https://apps-afsc.fisheries.noaa.gov/refm/docs/2020/BSAIrocksole.pdf.

Meredith, M., Sommerkorn, M., Cassotta, S., Derksen, C., Ekaykin, E., Hollowed, A., Kofinas, G., Mackintosh, A., Melbourne-Thomas, J., Muelbert, M.M.C., Ottersen, G.,

Pritchard, H., Schuur, E.A.G., 2019. Polar regions. In: Pörtner, H.-O., Roberts, D.C., Masson-Delmotte, V., Zhai, P., Tignor, M., Poloczanska, E., Mintenbeck, K., Alegría, A., Nicolai, M., Okem, A., Petzold, J., Rama, B., Weyer, N.M. (Eds.), IPCC Special Report on the Ocean and Cryosphere in a Changing Climate, pp. 203–320. https://www.ipcc.ch/srocc/.

Moore, C., 2014. Welfare estimates of avoided ocean acidification in the U.S. mollusk market. J. Agric. Resour. Econ. 40, 1–13.

Mueter, F., Bouchard, C., Hop, H., Laurel, B., Norcross, B., 2020. Arctic gadids in a rapidly changing environment. Polar Biol. 43, 945–949.

Myers, R.A., 1998. When do environment-recruitment correlations work. Rev. Fish Biol. Fish. 8, 285–305.

Narita, D., Poertner, H.O., Rehdanz, K., 2020. Accounting for risk transitions of ocean ecosystems under climate change: an economic justification for more ambitious policy responses. Climatic Change 162, 1–11.

Oliver, E.C.J., Donat, M.G., Burrows, M.T., Moore, P.J., Smale, D.A., Alexander, L.V., Benthuysen, J.A., Feng, M., Sen Gupta, A., Hobday, A.J., Holbrook, N.J., Perkins-Kirkpatrick, S.E., Scannell, H.A., Straub, S.C., Wernberg, T., 2018. Longer and more frequent marine heatwaves over the past century. Nat. Commun. 9, 1–12.

Pacific Fishery Management Council (PFMC), 2020. Terms of reference for the groundfish and coastal pelagic species stock assessment review process for 2021-2022. In: https://www.pcouncil.org/documents/2021/01/terms-of-reference-for-the-coastal-pelagic-species-stock-assessment-review-process-for-2021-2022-december-2020.pdf/.

Pennington, M., Volstad, J.H., 1994. Assessing the effect of intra-haul correlation and variable density on estimates of population characteristics from marine surveys. Biometrics 50, 725–732.

Piatt, J.F., Parrish, J.K., Renner, H.M., Schoen, S.K., Jones, T.T., Arimitsu, M.L., Kuletz, K.J., Bodenstein, B., García-Reyes, M., Duerr, R.S., Corcoran, R.M., Kaler, R. S.A., McChesney, G.J., Golightly, R.T., Coletti, H.A., Suryan, R.M., Burgess, H.K., Lindsey, J., Lindquist, K., Warzybok, P.M., Jahncke, J., Roletto, J., Sydeman, W.J., 2020. Extreme mortality and reproductive failure of common murres resulting from the northeast Pacific marine heatwave of 2014-2016. PloS One 15. https://doi.org/10.1371/journal.pone.0226087.

Pilcher, D.J., Naiman, D.M., Cross, J.N., Hermann, A.J., Siedlecki, S.A., Gibson, G.A., Mathis, J.T., 2019. Modeled effect of coastal biogeochemical processes, climate variability, and ocean acidification on aragonite saturation state in the Bering sea. Front. Mar. Sci. 5, 508. https://doi.org/10.3389/fmars.2018.00508.

Plagányi, É.E., 2007. Models for an Ecosystem Approach to Fisheries. FAO Fish Tech. Pap 477. 108pp. http://www.fao.org/3/a-a1149e.pdf.

Privitera-Johnson, K.M., Punt, A.E., 2020. Leveraging scientific uncertainty in fisheries management for estimating among-assessment variation in overfishing limits. ICES J. Mar. Sci. 77, 515–526.

Punt, A.E., Poljak, D., Dalton, M.G., Foy, R.J., 2014. Evaluating the impact of OA on fishery yields and profits: the example of red king crab in Bristol Bay. Ecol. Model. 285, 39–53.

Punt, A.E., Dalton, M.G., Foy, R.J., 2020. Multispecies yield and profit when exploitation rates vary spatially including the impact on mortality of ocean acidification on North Pacific crab stocks. Fish. Res. 225, 105481.

Punt, A.E., Foy, R.J., Dalton, M.G., Long, W.C., Swiney, K.M., 2016. Effects of long-term exposure to ocean acidification conditions on future southern Tanner crab (Chionoecetes bairdi) fisheries management. ICES J. Mar. Sci. 73, 849–864.

Ralston, S., Punt, A.E., Hamel, O.S., DeVore, J., Conser, R.J., 2011. An approach to quantifying scientific uncertainty in stock assessment. Fish. Bull. 109, 217–231.

Reum, J.C.P., Blanchard, J.L., Holsman, K.K., Aydin, K., Hollowed, A.B., Hermann, A.J., Cheng, W., Faig, A., Haynie, A.C., Punt, A.E., 2020. Ensemble projections of future climate change impacts on the eastern Bering sea food web using a multispecies size spectrum model. Front Mar Sci 7. https://doi.org/10.3389/fmars.2020.00124.

Rheuban, J.E., Doney, S.C., Cooley, S.R., Hart, D.R., 2018. Projected impacts of climate change, ocean acidification, and management on the US Atlantic sea scallop (*Placopecten magellanicus*) fishery. PloS One 13, e0203536. https://doi.org/10.1371/journal.pone.0203536.

Santora, J.A., Mantua, N.J., Schroeder, I.D., Field, J.C., Hazen, E.L., Board, S.J., Sydeman, W.J., Wells, B.K., Calambokidis, J., Saez, L., Lawson, D., Forney, K.A., 2020. Habitat compression and ecosystem shifts as potential links be- tween marine heatwave and record whale entanglements. Nat. Commun. 11, 536.

Schirripa, M.J., Goodyear, C.P., Methot, R.M., 2009. Testing different methods of incorporating climate data into the assessment of US West Coast sablefish. ICES J. Mar. Sci. 66, 1605–1613.

Siddon, E.C., Kristiansen, T., Mueter, F.J., Holsman, K.K., Heintz, R.A., Farley, E.V., 2013. Spatial match-mismatch between juvenile fish and prey provides a mechanism for recruitment variability across contrasting climate conditions in the eastern Bering Sea. PloS One 8, e84526. https://doi.org/10.1371/journal.pone.0084526.

Seung, C.K., Dalton, M.G., Punt, A.E., Poljak, D., Foy, R.J., 2015. Economic impacts of changes in a crab fishery from ocean acidification. Clim. Chang. Econ. 6 https://doi.org/10.1142/S2010007815500177.

Sigler, M.F., Napp, J.M., Stabeno, P.J., Heintz, R.A., Lomas, M.W., Hunt, G.L., 2016. Variation in annual production of copepods, euphausiids, and juvenile walleye pollock in the southeastern Bering Sea. Deep Sea Res. II 134, 223–234.

Smale, D.A., Wernberg, T., Oliver, E.C.J., Thomsen, M., Harvey, B.P., Straub, S.C., Burrows, M.T., Alexander, L.V., Benthuysen, J.A., Donat, M.G., Feng, M., Hobday, A. J., Holbrook, N.J., Perkins-Kirkpatrick, S.E., Scannell, H.A., Sen Gupta, A., Payne, B. L., Moore, P.J., 2019. Marine heatwaves threaten global biodiversity and the provision of ecosystem services. Nat. Clim. Change 9, 306–312.

Spencer, P.D., Holsman, K.K., Zador, S., Bond, N.A., Mueter, F.J., Hollowed, A.B., Ianelli, J.N., 2016. Modelling spatially dependent predation mortality of eastern Bering Sea walleye pollock, and its implications for stock dynamics under future climate scenarios. ICES J. Mar. Sci. 73, 1330–1342.

Spiegelhalter, D.J., Best, N.G., Carlin, B.P., Van Der Linde, A., 2002. Bayesian measures of model complexity and fit. J. Roy. Stat. Soc. B 64, 583–639.

Spies, I., Gruenthal, K.M., Drinan, D.P., Hollowed, A.B., Stevenson, D.E., Tarpey, C.M., Hauser, L., 2020. Genetic evidence of a northward range expansion in the eastern Bering Sea stock of Pacific cod. Evol. Appl. 13, 362–375.

Stevenson, D.E., Lauth, R.R., 2019. Bottom trawl surveys in the northern Bering Sea indicate recent shifts in the distribution of marine species. Polar Biol. 42, 407–421.

Swiney, K.M., Long, W.C., Foy, R.J., 2016. Effects of high pCO2 on Tanner crab reproduction and early life history, Part I: long-term exposure reduces hatching success and female calcification, and alters embryonic development. ICES J. Mar. Sci. 73, 825–835.

Szuwalski, C., Cheng, W., Foy, R., Hermann, A., Hollowed, A., Holsman, K., Lee, J., Stockhausen, W., Zheng, J., 2021. Climate change and the future productivity and distribution of crab in the Bering Sea. ICES J. Mar. Sci. 78, 502–515.

Taylor, K.E., Stouffer, R.J., Meehl, G.A., 2012. An overview of CMIP5 and the experiment design. Bull. Am. Meteorol. Soc. 93, 485–498.

Thorson, J.T., Arimitsu, M.L., Barnett, L.A.K., Cheng, W., Eisner, L.B., Haynie, A.C., Hermann, A.J., Holsman, K., Kimmel, D.G., Lomas, M.W., Richar, J., Siddon, E.C., (in press). Forecasting community reassembly using climate-linked spatio-temporal ecosystem models. Ecography 44, 612–625.

Turner, M.G., Calder, W.J., Cumming, G.S., Hughes, T.P., Jentsch, A., LaDeau, S.L., Lenton, T.M., Shuman, B.N., Turetsky, M.R., Ratajczak, Z., Williams, J.W., Williams, A.P., Carpenter, S.R., 2020. Climate change, ecosystems and abrupt change: science priorities. Phil. Trans. Roy. Soc. B 375, 20190105. https://doi.org/10.1098/rstb.2019.0105.

Wang, M., Overland, J.E., 2015. Projected future duration of the sea-ice-free season in the Alaskan Arctic. Prog. Oceanogr. 136, 50–59.

Wang, M., Yang, Q., Overland, J.E., Stabeno, P., 2018. Sea-ice cover timing in the Pacific Arctic: the present and projections to mid-century by selected CMIP5 models. Deep-Sea Res. II. 152, 22–34.

Watanabe, S., 2013. A widely applicable Bayesian information criterion. J. Mach. Learn. 14, 867–897.

Whitehouse, G.A., Aydin, K.Y., Hollowed, A.B., Holsman, K.K., Cheng, W., Faig, A., Haynie, A.C., Hermann, A.J., Kearney, K.A., Punt, A.E., Essington, T.E., 2021. Bottom-up impacts of forecasted climate change on the eastern Bering Sea food web. Front. Mar Sci. 8, 624301.